ABSTRACT

Title of Thesis: MORPHOLOGY OF CELLULOSE AND CELLULOSE BLEND THIN FILMS

Rui Lu, Master of Materials Science, 2017

Thesis Directed By: Professor and Associate Dean, Robert M. Briber
Department of Materials Science and Engineering

Cellulose is the most abundant, renewable, biocompatible and biodegradable natural polymer. Cellulose exhibits excellent chemical and mechanical stability, which makes it useful for applications such as construction, filtration, bio-scaffolding and packaging. It is useful to study amorphous cellulose as most reactions happen in the non-crystalline regions first and at the edge of crystalline regions. In this study, amorphous thin films of cotton linter cellulose with various thicknesses were spincoated on silicon wafers from cellulose solutions in dimethyl sulfoxide / ionic liquid mixtures. Optical microscopy and atomic force microscopy indicated that the morphology of as-cast films was sensitive to the film preparation conditions. A sample preparation protocol with low humidity system was developed to achieve featureless smooth films over multiple length scales from nanometers to tens of microns. X-ray reflectivity, X-ray diffraction, Fourier transform infrared spectroscopy and high resolution sum-frequency generation vibrational spectroscopy were utilized to confirm that there were no crystalline regions in the films.

One- and three- layer models were used to analyze the X-ray reflectivity data to obtain information about roughness, density and interfacial roughness as a function of film thickness from 10-100nm. Stability tests of the thin films were conducted under harsh conditions including hot water, acid and alkali solutions. The stability of thin films of cellulose blended with the synthetic polymer, polyacrylonitrile, was also investigated. The blend thin films improved the etching resistance to alkali solutions and retained the stability in hot water and acid solutions compared to the pure cellulose films.

MORPHOLOGY OF CELLULOSE AND CELLULOSE BLEND THIN FILMS

by

Rui Lu

Thesis submitted to the Faculty of the Graduate School of the
University of Maryland, College Park, in partial fulfillment
of the requirements for the degree of
[Master of Science]
[2017]

Advisory Committee:
Professor Robert M. Briber, Chair
Professor Lourdes G. Salamanca-Riba
Associate Professor Liangbing Hu

DEDICATION

To my parents, Dr. Howard Wang, Dr. Xin Zhang, Dr. Guangcui Yuan

and Wonseok Hwang for their encouragement and support.

ACKNOWLEDGEMENT

I would like to express my sincere gratitude and appreciation to many people for their support of the project and this master thesis. I wish to thank deeply my advisor Dr. Robert M. Briber for his insight in resolving many of the problems throughout my work and his patience during this study. Also, I would like to thank Dr. Howard Wang for guiding me the project and providing all the valuable suggestions and help. Many thanks go to Dr. Xin Zhang, who has been a great colleague and teacher and supported me and my work. He has also given me encouragement and suggestions beyond the academic field. Dr. Guangcui Yuan at NIST has advised me on X-ray reflectivity data analysis, encouraged me to solve the problems, and offered endless support. I wish to appreciate the help of Wonsoek Hwang who helped me with learning many instruments. I also appreciate all other members of our group during my research and thesis writing.

I would like to thank my committee members, Dr. Lourdes G. Salamanca-Riba and Dr. Liangbing Hu for their patience and support.

Finally, I would like to express my appreciation to my dearest parents, for their long-standing love, support and sacrifice.

TABLE OF CONTENTS

List of Tables

List of Figures

Chapter 1: Introduction

1.1 Cellulose Background

1.1.1 Amorphous versus Crystalline Cellulose

Cellulose is a renewable, non-toxic, biocompatible and biodegradable natural polymer, and the most abundant polymer in the world. Cellulose can be obtained from plants in many forms like wood pulp, cotton and leaves etc. It has been widely used in items such as paper products, fibers, biofuel, membranes and coatings etc. [1]

Native cellulose has the cellulose crystalline type I structure, the most common form of all the crystal forms of cellulose, including I_α and I_β shown in Figure 1.1. Cellulose in the form of structure I_α can be derived from algae and bacteria and has a triclinic unit cell structure with a = 6.717 Å, b = 5.962 Å, c = 10.400 Å, $\alpha = 118.08°$, $\beta = 114.80°$ and $\gamma = 80.37°$. Cellulose type I_β is found in higher plants and has a monoclinic unit cell structure with a = 7.784 Å, b = 8.201 Å, c = 10.38 Å, $\alpha = \beta = 90°$ and $\gamma = 96.5°$. [2] Cellulose II is found in cellulose regenerated from solutions of cellulose I [3].

Cellulose is a linear polymer of D-glucose with each repeating unit comprising two anhydroglucose rings $(C_6H_{10}O_5)_n$ connected by an oxygen atom at C1 on one ring and C4 on the other ring to form a β glycosidic bond at position 1-4 as shown in Figure 1.2. There are three kinds of bonds in the cellulose crystals, the first kind are the covalent bonds along the chain, the second are hydrogen bonds such as -C**OH** · · · -C**O**H, -C**OH** · · · $\mathbf{O}_{ring}$, and the third is Van der Waals interactions (-C**H** · · ·**O**, -C**H** · · ·**C)**. The –OH and O on the ring form hydrogen bonds on the chain inside the sheet and between

layers shown in Figure 1.3, which lends to the hydrophobic interaction between the layers and the hydrophilic interaction associated with -OH groups on the rings [4].

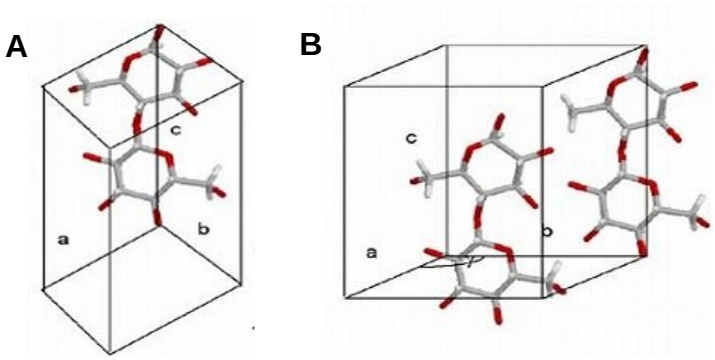

Figure 1.1 Structure of (A) cellulose I_α with triclinic one chain unit cell; (B) cellulose I_β with monoclinic two chain unit cell. [5]

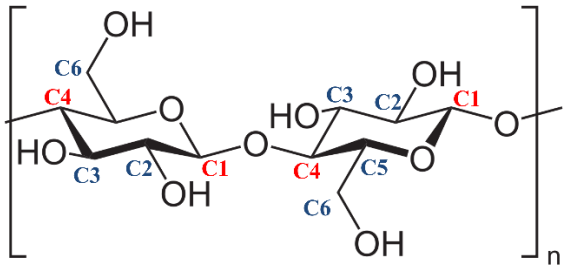

Figure 1.2 Cellulose molecular structure unit with carbons labeled.

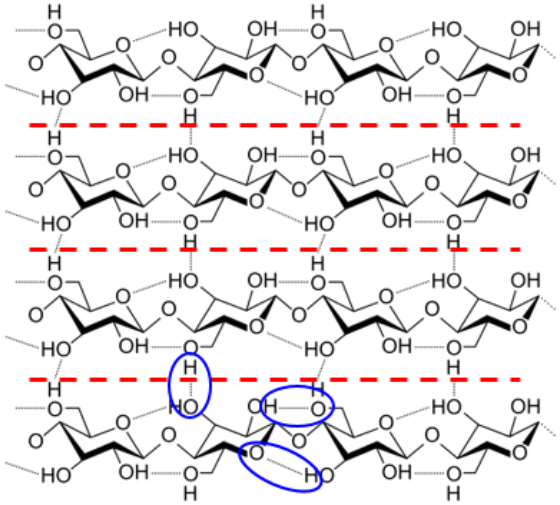

Figure 1.3 The –OH and O_{ring} form hydrogen bonds on the chain inside the sheet shown by blue circles and between layers presented by red dotted lines.

Crystalline and amorphous domains coexist in most cellulose materials [6]. Crystalline cellulose can be transformed to the amorphous state under 250MPa pressure at 320˚C in water without the presence of other chemicals [7]. Due to the differing proportions and organization of the crystalline regions and non-crystalline regions in cellulose from different sources, the mechanical properties are different from one type of cellulose to another [8]. There are differences between the hydrogen bonding in the crystalline and amorphous regions [3]. The amorphous regions are the most reactive component in cellulose, followed by the edges of the crystalline regions. The internal crystalline regions have relatively low reactivity. [9] Many applications require using the reactivity of cellulose and much research has been done on finding effective methods for dissolution of cellulose [10-13].

1.1.2 Cellulose Composites

There are a number of forms of regenerated cellulose currently in use for fibers, films and gels etc. covering a range of applications. Cellulose alone as a material cannot meet requirements for certain products that require electric conductivity, magnetic properties or fluorescence etc. A cellulose blend material is a possible choice to enable a broader range of applications.

Cellulose can be used as a component in composites by creating solutions of the blend and produce the regenerated composite by removing the solvent. Examples in the literature include preparing cellulose/polyethylene glycol (PEG) blends using NaOH/ urea solutions [14], cellulose/graphite oxide blends from in NaOH/ urea aqueous solutions [15], and cellulose/Fe_3O_4 blends in 1-ethyl-3-methylimidazolium chloride (EMIM Cl)

solution [16]. Another example is making solutions of the different components and achieving the composite by combining the solutions during the regeneration process. Linhardt and coworkers obtained conductive cellulose/multi-walled carbon nanotubes (MWNT) fibers by dissolving cellulose and MWNT in separate ionic liquid solutions and spinning fibers with MWNT as the core first and continuing spinning with cellulose as the protective sheath regenerated from the solution [17]. A third method is to prepare the regenerated cellulose and attach the other material. For instance, Au, Fe_2O_3, metal ions and dyes etc. can be synthesized as nanoparticles and attached to regenerated cellulose products [18-21].

1.1.3 Cellulose Solutions

The process of making cellulose solutions has been established for over 100 years [22]. For many decades, the viscose process for cellulose dissolution has been popular. CS_2 was utilized for cellulose to produce cellulose xanthogenate. The cellulose xanthogenate could be dissolved in aqueous NaOH to form a viscose solution and the regenerated cellulose could be obtained when an acidic solution was introduced. This method causes environmental problems such as liquid waste and emitted CS_2 and H_2S gas [13]. Research has been on going to find environmentally friendly solvents for cellulose. The main requirement to dissolve cellulose is the effective and rapid breaking of hydrogen bonds within the cellulose structure.

In 1969, N-Methylmorpholine N-oxide (NMMO) was discovered for dissolving cellulose as a “green” organic solvent with no harmful derivatives and it can be recycled and reused [11]. The dissolution process first happens in the amorphous regions with the

disruption of the hydrogen bonds by NMMO, and then the dipole group N ⟶ O in NMMO could form new hydrogen bonds with cellulose hydroxyl groups as complexes. This gradually breaks down the crystalline regions and completes the dissolution process [23]. NMMO was found to be more likely to form hydrogen bonds with water molecules instead of cellulose. NMMO•2.5 H_2O hydrates cannot dissolve cellulose since all the possible hydrogen bond positions are taken by H_2O. The high melting temperature of 457K for NMMO are required and heating process would cause degradation of cellulose and NMMO, making pure NMMO an undesirable solvent for cellulose. As a compromise, NMMO•H_2O hydrate was considered as an appropriate solvent for cellulose as it has a melting temperature of 358K. An antioxidant is needed to stabilize the system as NMMO can be easily oxidized and may explode during transportation and storage [24].

In 1934, Graenacher found that the ionic liquid of molten N-ethylpyridinium chloride could dissolve cellulose [10]. At that time, due to its high melting temperature and the lack of general knowledge on ionic liquids (ILs), this idea was not fully explored. In 2002, ILs were found to be a simple and efficient solvent for the dissolution of cellulose by Roger and his coworkers [12]. The discovery opened a new approach to the dissolution of cellulose. There are many choices for the anions and cations that make up ILs and many researchers investigated the mechanism of how cellulose interacted with IL ions [25-28]. It is commonly agreed that the anions in ILs first break the cellulose hydrogen bonds, then strongly form coupling with hydroxyl groups as negatively charged complexes as discussed by Moulthrop, Remsing and others using high resolution ^{13}C NMR [29-31]. Wang, Singh and coworkers reported that after the anions disrupted the hydrogen bonds, the cations could penetrate inside the bulk cellulose and form hydrogen bonds with -OH and

other oxygen atoms in the cellulose network while keeping apart the small sections caused by the initial anion disruption [32,33].

As the investigation of cellulose dissolution systems developed, several other systems were discovered including alkali/urea or thiourea aqueous solution, LiCl/DMAc system, and molten inorganic salt hydrates. [22]

1.2 Cellulose and Cellulose Blend Thin Films

1.2.1 Cellulose

Regenerated cellulose has been used in various forms such as fibers, powder, films, gels and microspheres etc. with excellent thermal, chemical, mechanical stability as well as biocompatibility, biodegradability and renewability.

We aim to produce amorphous ultra-thin films of cellulose and composites from molecular solution through a facile and quick processing system by efficiently dissolving cellulose with both hydrophilic and hydrophobic polymers without causing any derivatizing reactions.

Producing amorphous cellulose thin films is a significant challenge because due to water molecules in air, the amorphous cellulose may partially crystallize into cellulose II, especially with hydroscopic ILs and dimethyl sulfoxide (DMSO) used as solvent in the solution. In this work, a simple method was developed to reduce the effect of moisture.

Kontturi and others prepared ultrathin cellulose films (20nm) by spincoating toluene/trimethylsilyl cellulose (TMSC) (10 g/dm^3) solution on silicon substrate and exposing the film to the vapor of 2 M hydrochloric acid (HCl) for 1 minute to ensure the transformation of TMSC to cellulose. Diffraction patterns possibly due to very small

crystallites of cellulose II or III_1 were detected by grazing incidence X-ray diffraction (GIXRD), so the films were regarded as mostly amorphous state. [34] Zhang and coworkers achieved excellent transparent amorphous cellulose films regenerated from lithium chloride (LiCl)/N,N dimethylacetamide (DMAc) solution by acetone with thicknesses from 16 to 29 μm. An applicator was used to control the cellulose film thickness and cast the solution on glass plates. And the particle size of the cellulose sources used in their work effects the amorphousness of the cellulose films and more perfect amorphous cellulose films were obtained from Whatman CF11 fibrous medium cellulose powder (50–350 μm, GE Healthcare Life Science Corp). [35]

1.2.2 1-Ethyl-3-Methylimidazolium Acetate and Dimethyl Sulfoxide

IL are defined as a group of salts consisting of ions and short-lived ion pairs with a melting point lower than 373K [36]. ILs have useful properties such as excellent solvating ability, thermal stability, strong polarity, negligible vapor pressure and non-flammability [37]. There are three typical ILs generally used with cellulose and discussed by researchers, 1-ethyl-3-methylimidazolium acetate (EMIM Ac) [38], 1-butyl-3-methylimidazolium chloride (BMIM Cl) [25] and 1-allyl-3-methylimidazolium chloride (AMIM Cl) [30]. Kosan and coworkers found that with the relatively small EMIM cation, there was improved interaction with cellulose and lower viscosity of the resultant solutions which resulted in a higher cellulose dissolution concentrations [38].

Using only IL to dissolve cellulose can result in a very viscous or gel-like solution that is not desirable for making thin films of cellulose, so finding a good solvent system for dilute solutions is required. A polar aprotic solvent for both polar and nonpolar

compounds is suitable for the non-aqueous cellulose material and can form hydrogen bonds by accepting hydrogen and dipole-dipole associations [39]. Compared to other similar aprotic solvents, dimethyl sulfoxide (DMSO) has less toxicity than dimethylformamide (DMF) and N,N-dimethylacetamide (DMA), etc. [40] Most organic solvents as well as water are miscible with DMSO so it is important to remove any water in DMSO. Type 3A molecular sieves do not react with DMSO and can be used to absorb water from DMSO.

1.2.3 Polyacrylonitrile

Polyacrylonitrile (PAN) has wide range of applications for fibers, filtration membranes, and electronics etc. because of the non-toxicity, excellent mechanical properties, good hydrophobicity and environmentally friendly characteristics [41,42]. After the polymerization of the monomer acrylonitrile, a semicrystalline synthetic thermoplastic resin PAN is obtained with high hardness, high stiffness and good resistance to most solvents and chemicals due to the strong hydrogen bond interactions between the nitrile (CN) groups. The polar CN groups affect the electrical, mechanical and thermal properties of PAN and a strong hydrogen bonding solvent is required for dissolution [43].

PAN is widely used because of the advantages of chemical stability and high water permeation rate [44]. PAN is often mixed with other materials to obtain special properties like PAN and carbon nanotube (CNT) composite films which exhibited electrical conductivities up to 5500 S/m and increasing tensile modulus and tensile strength [45]. Polyvinyl acetate (PVA)/PAN blend films prepared from solution in DMSO showed

stronger hydrophobicity than pure PVA films, increased tensile strength with the increase of the PAN mole ratio, decreased melting temperature and degradation of the composite films [46]. Films made from a blend of chitosan and PAN can strongly increase the sorption capacity of metal ions from waste water [47]. The polymer blend of PAN/polymethyl methacrylate (PMMA)/polystyrene (PS) is a promising electrolyte for lithium ion batteries [48].

1.2.4 Mixture of Cellulose and Polyacylonitrile

Cellulose and PAN blends were prepared by mixing separate clear solutions of PAN and cellulose and then spincoating as flat films. IL (EMIM Ac) and aprotic solvent (DMSO) comprise an effective solvent system that dissolves both cellulose and PAN. PAN is completely soluble in DMSO at room temperature. Cellulose can be dissolved in DMSO / EMIM Ac mixture at 363 K. These solutions can then be mixed to obtain the blend solution [42,49].

1.3 Characterization Measurements

1.3.1 X-ray Reflectometry

X-ray reflectometry (XRR) is a useful analytical X-ray scattering technique for characterization of thin films, surfaces and multilayers. It is a non-destructive and surface-sensitive method for both crystalline and amorphous materials.

A highly-focused incident X-ray beam is reflected from a flat sample surface and interfaces. The two reflected X-rays in the specular direction interfere with each other to produce a reflectometry pattern with Kiessig fringes (reflected angle equals to incident

angle). The oscillations in the reflected X-ray beam are used to determine layer thickness, density, roughness and interstitial roughness of multilayer thin films by collecting data as shown in Figure 1.4.

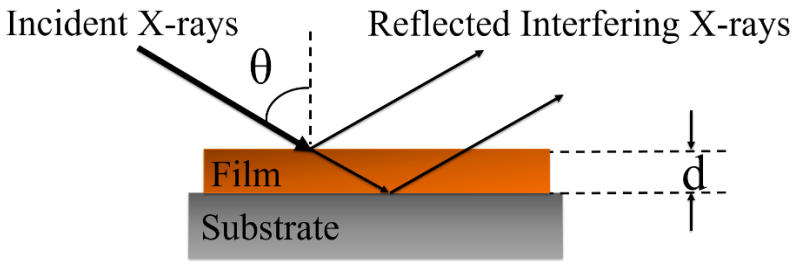

Figure 1.4 Diagram of x-ray reflectometry.

1.3.2 X-ray Diffraction

X-ray diffraction (XRD) is also a non-destructive characterization method of material properties for the periodic atomic structure of crystals. Part of the X-ray incident beam will be scattered by the atomic planes of the crystal and interfere with each other as they leave the crystal. The collected diffraction data can lead to qualitative and quantitative phase analysis using Bragg's law as the basis understanding the structure, shape and internal stress of the crystalline regions shown in Figure 1.5. It is a useful tool to determine the crystal structure of the cellulose in this study.

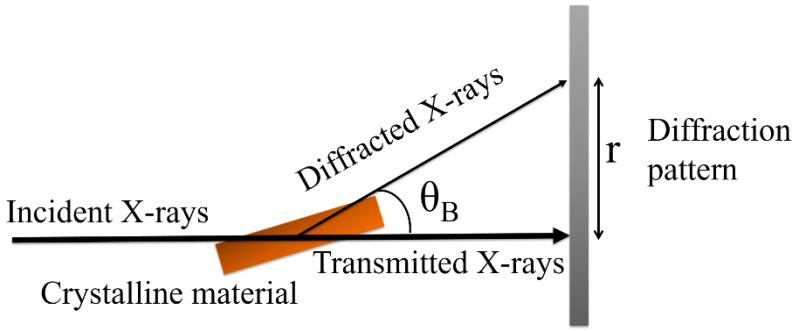

Figure 1.5 Diagram of x-ray diffraction.

1.3.3 High Resolution Sum-Frequency Generation Vibrational Spectroscopy

Sum-frequency generation vibrational spectroscopy (SFG-VS) due to the second order nonlinear process, is highly sensitive to the symmetry in the structure of molecular assemblies. SFG-VS can detect basic crystalline structures and polymorphism of crystalline material. For amorphous material, only signals of surface or interfaces can be detected and collected. [50]

The spectra of SFG-VS are generated by simultaneous interaction (presented as Eq. 1.1) between a visible or near-infrared laser beam with frequency ω_{vis} and an infrared (IR) laser beam with frequency ω_{IR}. Fixing the visible laser beam with frequency ω_{vis} and tuning the IR beam frequencies ω_{IR}, the SFG spectra can be collected by a charge coupled device (CCD) detector. The spectrum intensity is a function of ω_{SFG}.

$$\omega_{SFG} = \omega_{vis} + \omega_{IR} \qquad \text{(Eq. 1.1)}$$

1.3.4 Fourier Transform Infrared Spectroscopy

Fourier transform infrared spectroscopy (FTIR) is a tool to identify unknown materials or components in a mixture. It detects the frequencies of vibrations between the bonds of the atoms that are signature for each material due to the unique combination of atoms present. FTIR can be used to identify the amount of components qualitatively as the size of the peaks in the spectrum can be analyzed.

A beam splitter is a key factor in FTIR instrument in Figure 1.6. It splits the incident infrared (IR) beam into two optical beams. One beam is reflected by a fixed mirror, the other one is reflected by a moving mirror over a very short range (typically a few millimeters). The recombined IR beams either are absorbed by the sample or transmit

through the sample. The final spectrum produced after Fourier transformation is yielding a unique molecular fingerprint for each kind of material.

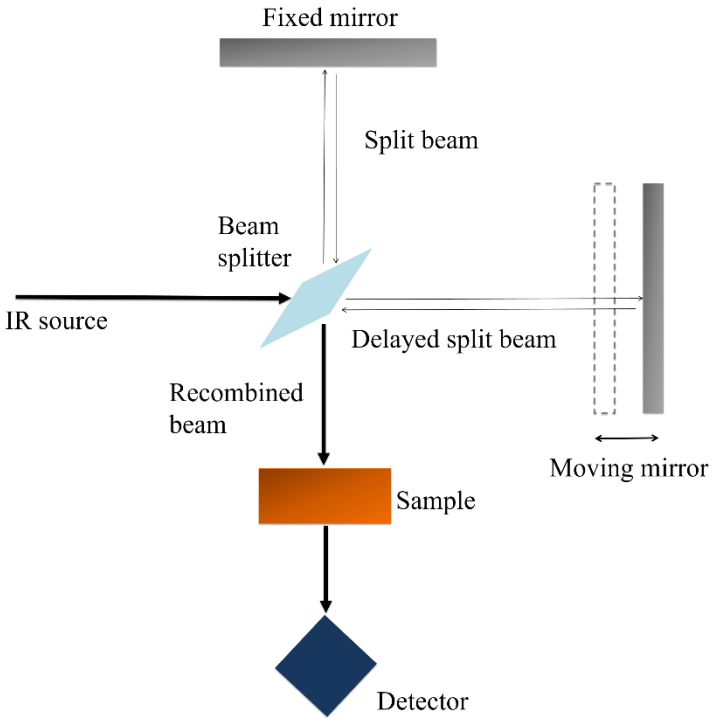

Figure 1.6 Diagram of Fourier transform infrared spectroscopy.

1.4 Thesis Objectives

This research is aimed at preparing clear molecular solutions of cellulose and cellulose blends with PAN in an IL and aprotic solvent system. The solutions were used to spincoat fully amorphous cellulose thin films as a function of thicknesses from less than 10 nm to 100 nm while keeping the RMS roughness less than 2 nm. Models to fit XRR data were built to analyze the thickness, roughness and density of the thin films. The thin films examined to determine the resistance to harsh conditions such as hot

water, acidic and base solutions. Cellulose and PAN blend thin films were made for comparison to pure cellulose thin films.

Chapter 2: Cellulose Thin Film

2.1 Introduction

Cellulose is a promising material for new applications due to its abundant presence in nature and its relative stability against oxidation and chemical degradation [51]. Cellulose is comprised of crystalline regions and amorphous regions and generally most reactions occur first in the amorphous region lack of order and lower density. The work presented here solved the difficulty in producing amorphous cellulose thin films under normal experimental conditions. The ability to produce amorphous cellulose thin films at the single nanometer scale was also investigated.

The mass density for amorphous regions is 1.5 g/cm^3 versus 1.588 g/cm^3 for crystalline cellulose. Much of the work on cellulose dissolution systems that have been used to prepare regenerated cellulose has focused on the regenerated products with crystalline regions, while little work has been done on fully amorphous cellulose. This chapter demonstrates a method of preparing fully amorphous cellulose thin films of different thicknesses using the same general spincoating procedure.

Amorphous glassy cellulose thin films were prepared from DMSO / IL molecular solutions by spincoating in dry N_2 gas (to keep the humidity as low as possible). Films with various thicknesses ranging from less than 10 nm to about 100 nm were carefully prepared while maintaining the roughness at the nanometer scale. Measurements by X-ray diffraction (XRD), X-ray reflectometry (XRR), high resolution sum-frequency generation vibrational spectroscopy (HR-SFG-VS) and Fourier transform infrared spectroscopy (FTIR) confirmed the film was fully amorphous.

The stability of cellulose film was tested by soaking in various harsh solvents including hydrochloric acid (HCl), sodium hydroxide (NaOH), NaOH/urea solution, hot water and organic solvents.

2.2 Experimental

2.2.1 Apparatus

Humidity was found to lead to the formation of crystalline cellulose fibrils during spincoating. In order to produce regenerated amorphous cellulose thin films, a low humidity environment was required. Dry nitrogen was used to fill a glass bell jar on a spin coater. A special switching port in the middle of the bell jar was designed to inject solution onto the silicon substrate without lifting the bell jar as shown in Figure 2.1. Dry atmosphere was achieved for preparing these thin film samples using this system.

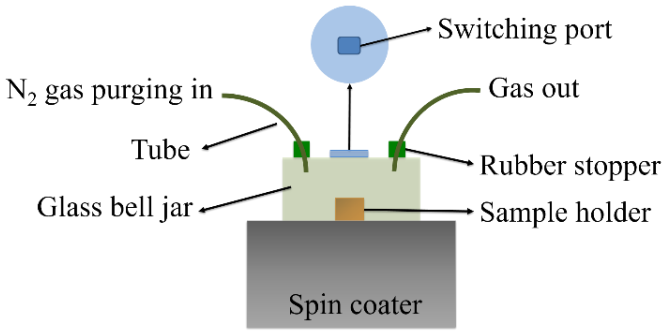

Figure 2.1 Schematic of the spincoating environmental chamber.

2.2.2 Cellulose Thin Film Preparation

All chemicals used in this research were dried to remove water. Microcrystalline cellulose Avicel PH101 purchased from Sigma Aldrich was put in vacuum at 333K for 12

hours and EMIM Ac for 2 hours respectively to remove any moisture. Reagent grade DMSO and other solvents used were dried with molecular sieves and stored in a low humidity glove box.

Molecular cellulose solutions were prepared using the following protocol. Microcrystalline cellulose Avicel PH101 was dispersed in DMSO with EMIM Ac added afterwards (all in a glove box) with the mole ratio of EMIM Ac: cellulose anhydroglucose unit (AGU) of 3:1. The solution was heated to 363K for 5 minutes and stirred vigorously to obtain a fully dissolved solution. The heating and stirring process was continued until the solution was clear.

Cellulose thin films were prepared by spinning the solution on a silicon wafer or a glass substrate in the low humidity apparatus described above. Before spinning, N_2 gas was purged into the glass bell jar and continued during spinning. Spin speed started at 1000 rpm for 5 minutes, then the spin speed was reduced to 100 rpm for 30 seconds during which a mixture of 1:1 weight ratio of anhydrous acetone and toluene was dripped continuously and gently onto the surface of the film to remove part of the DMSO and EMIM Ac. Finally, the spin speed increased to 500 rpm and the film was washed with acetone for 20 seconds and kept spinning for 40 more seconds to dry. After spinning, the film was vitrified and was capable of being exposed to air without subsequent crystallization occurring. The cellulose film was put in a vacuum oven at 333K to remove any residual DMSO, then soaked in fresh acetone 3 times (each time lasted 15 minutes) to remove residual EMIM Ac. The film preparation is finished by ethanol rinsing and drying with N_2.

2.3 Results and Discussion

2.3.1 Morphology and Composition Characterization

Cellulose thin films have been investigated by a number of groups using different dissolution systems and regeneration methods, however, rough films usually resulted due to humidity exposure or regeneration problems [34,52,53].

The advantage of the approach developed in this research is that it produces a flat amorphous cellulose film with smooth surface that is uniform across the film. The morphology of the cellulose films was characterized by atomic force microscopy (AFM) and optical microscopy which showed the films were flat, smooth and consistent over different thicknesses. The composition and structure of the film was studied by XRR, FTIR and HR-SFG-VS.

AFM height images of cellulose microcrystalline, cellulose thin films spincoated in air, and thin films of different concentration solutions spincoated in dry N_2 gas atmosphere are shown in Figure 2.2. Figure 2.2 A is the surface morphology of crystalline fibrils in an Avicel PH101 thin film spincoated from a 1 wt% stable water suspension on silicon wafer in air that was stirred vigorously and then left to settle for 2 hours resulting in a stable suspension before spincoating. The spincoated film was composed of small particles in Avicel PH101 powder. Figure 2.2 B shows crystalline fibrils on the surface of a cellulose thin film from a molecular solution spincoated in air, followed by vacuum removal of DMSO and then soaked in fresh acetone to remove EMIM Ac. The formation of the crystalline fibrils was the result of the humidity in air interacting with the cellulose solution during spincoating. Once these crystalline fibrils formed, the removal of DMSO and EMIM Ac could not reverse the crystallization.

Figure 2.2 C and Figure 2.2 D are AFM height images of thin films from 1 wt% and 2 wt% cellulose molecular solutions spincoated in a N_2 gas environment. As can be observed in the images, the surface of the two films are similar to each other with a root mean square (RMS) roughness of 0.644 nm and 1.05 nm for films of thicknesses of 29 nm and 88 nm respectively. This confirms the method produces flat films over a wide thickness range. Birefringence cannot be observed with cross polarized microscopy, indicating a possible amorphous film although it may also result from the thickness being too thin to produce significant birefringence.

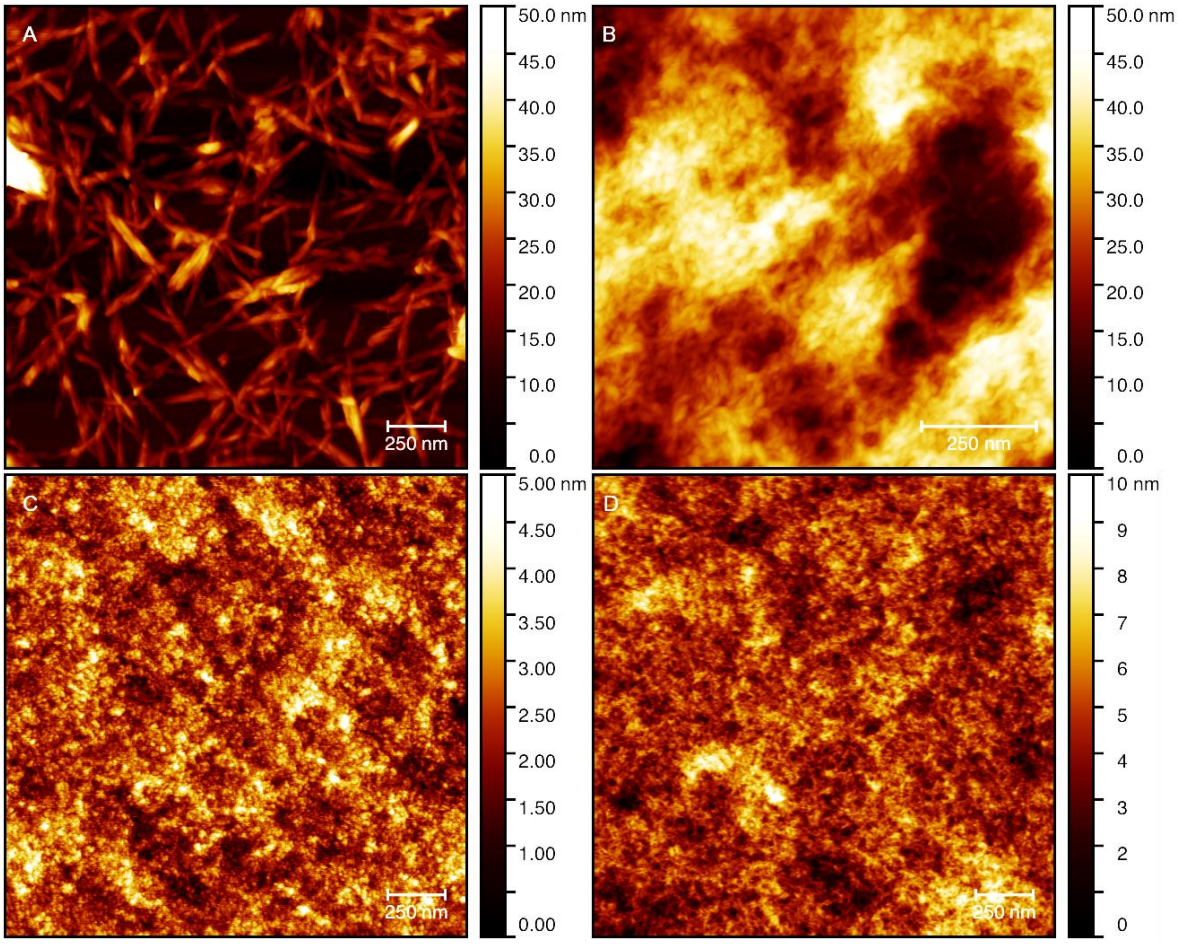

Figure 2.2 AFM images of cellulose films, (A) Avicel PH101 stable water suspension spincoated film in air with the crystalline fibers; (B) cellulose molecular solution spincoated film in air with fibril structures and rough surface; (C) 1 wt% cellulose solution spincoated film in dry N_2 gas with flat surface of RMS 0.644 nm; (D) 2 wt% cellulose solution spincoated film in dry N_2 gas with flat surface of RMS 1.05 nm.

FTIR spectra were obtained using Thermo Nicolet NEXUS 670 instrument. FTIR helped to confirm that IL was removed from the cellulose thin film prepared by the method described above.

Figure 2.3 shows the FTIR results (the spectra were scaled for comparison) from cellulose films (with same spincoating and vacuum process) soaked in acetone and ethanol respectively for EMIM Ac removal, Avicel PH101 powder and pure EMIM Ac for comparison. The sharp peak at 1580 cm^{-1} indicates the existence of EMIM Ac. It can be noticed that in pure EMIM Ac and cellulose thin film soaked in ethanol shows a strong peak at 1580 cm^{-1}, this means that ethanol is not an effective solvent to extract EMIM Ac from the cellulose film. However, EMIM Ac is soluble in water and alcohol. Ethanol soaking probably resulted in a dense surface layer because of the process of removing EMIM Ac. The dense surface layer may become a barrier to prevent ethanol from further dissolving EMIM Ac inside the cellulose film. For a cellulose thin film soaked in acetone, the disappearance of peak at 1580 cm^{-1} showed that acetone can fully remove EMIM Ac even though EMIM Ac is not highly soluble in acetone. Due to some bound water hydroxyl groups, FTIR peak of cellulose at 1640 cm^{-1} near the EMIM Ac peak at 1580 cm^{-1} was enhanced. [54] By constantly using fresh acetone to soak the cellulose film the EMIM Ac was fully removed.

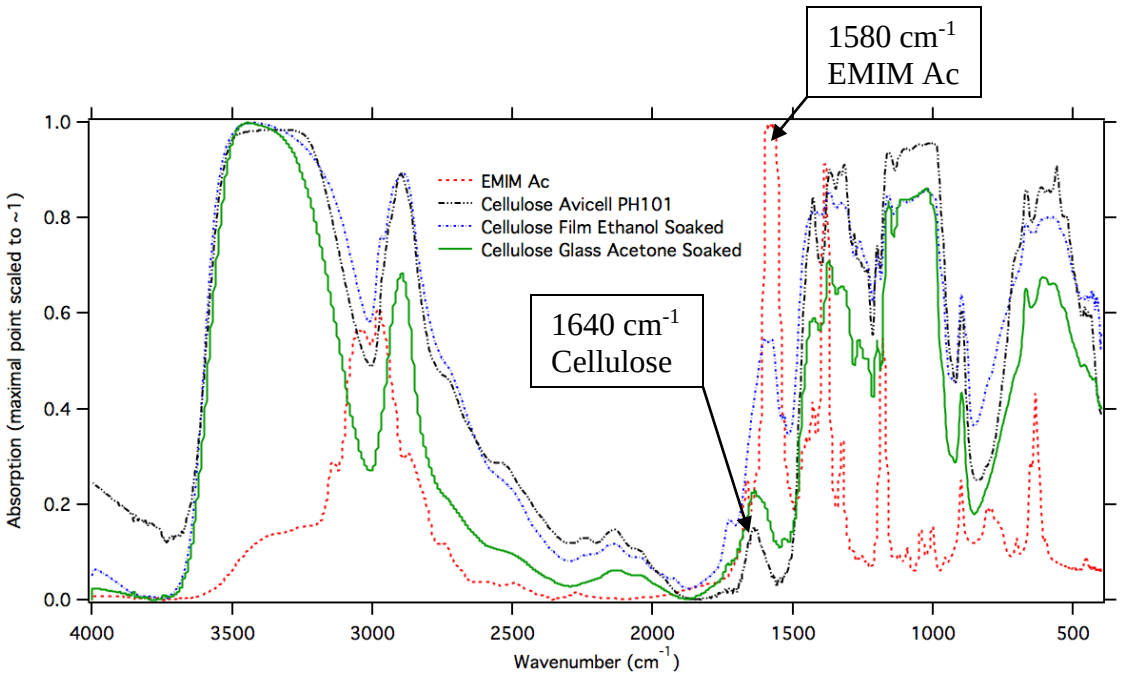

Figure 2.3 FTIR spectra of the Avicel PH101 powder, pure EMIM Ac, cellulose thin film soaked in acetone and cellulose thin film soaked in ethanol. The distinct peak of absorption in 1580 cm^{-1} is the indication of EMIM Ac existence in the films.

Figure 2.4 shows the XRD spectra of cellulose films made from two different sources measured using a Xenocs Xeuss 2.0 WAXS/SAXS system instrument, one curve is from Avicel PH101 microcrystalline powder purchased from Sigma Aldrich and the other is from filter paper. Thickness of all samples is less than 0.5 mm. Crystalline regions exist in both the filter paper and Avicel PH101 powder (pressed into a disc) which results in the high intensity narrow Bragg peaks shown by the blue and red solid lines. The data from the glassy cellulose shows only broad peaks indicating no crystalline order (both blue and red dotted lines of glassy cellulose were divided by a factor of 1.75 to make the baselines roughly the same level as the blue and red solid lines).

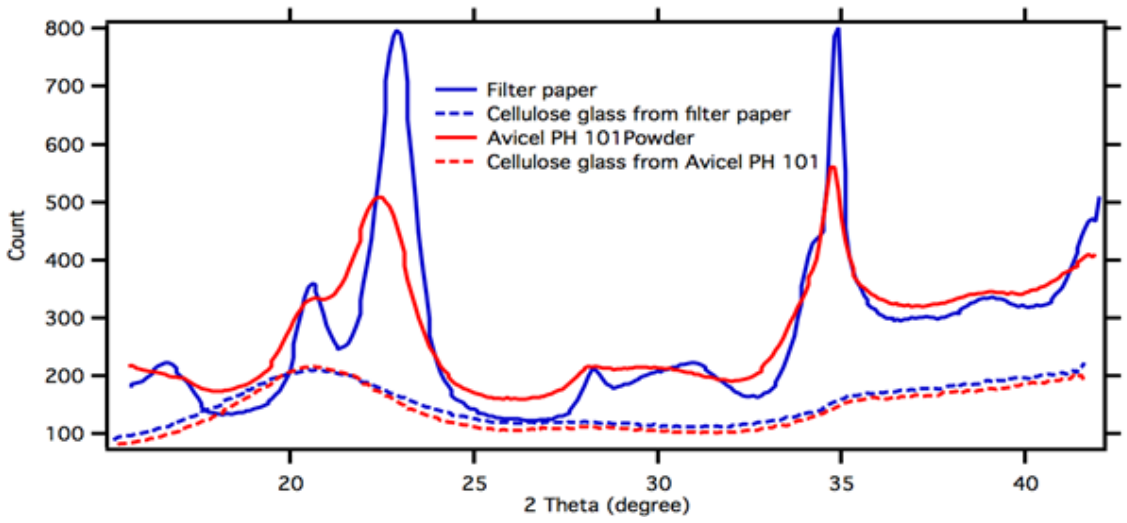

Figure 2.4 XRD spectra of the cellulose films made from Avicel PH101 powder and filter paper.

HR-SFG-VS was utilized to study different types of native cellulose with variations in polymorphism and can help determine the source of different cellulose samples. The C-H stretching can be used to detect cellulose I_α and I_β. This special technique provided a possibility to study cellulose in a more detailed way. [50] Li Fu and Hongfei Wang at Pacific Northwest National Lab helped to obtain the HR-SFG-VS spectrum.

HR-SFG-VS measurements shown in Figure 2.5 also confirmed the amorphous state of cellulose in the thin films through the C-H and O-H stretching vibration frequency regions. HR-SFG-VS is capable of measuring and analyzing crystallinity in cellulose as it can quantitatively provide the data of composition, interaction and orientational/ conformational structure as well as information on surfaces and interfaces [50,55]. The Avicel PH101 thin film was used as a reference for crystalline cellulose and showed distinct peaks at ~3325 cm^{-1} and ~2951 cm^{-1} which indicate the O-H hydrogen bonds and C-H stretch regions respectively [50]. The O-H stretching vibration peak at 3325 cm^{-1} acts differently in crystalline and amorphous cellulose. Within the crystalline region, the intra-

chain O(3)H-O(5) hydrogen bond is highly directional along the direction of cellulose crystal fibers. The 3325 cm^{-1} peak is not observed in amorphous cellulose because the intra-chain O(3)H-O(5) hydrogen bonds directionality gets disturbed. At 2951 cm^{-1}, the C-H stretch in Avicel PH101 occurs at position C(6) within the (002) plane in the forms of C(6)OH-O(2), O(2)H-OC(6) or C(6)OH-O(3) with high directionality [4]. In amorphous cellulose thin film, the 2951 cm^{-1} peak is not observed indicating that the hydrogen bonds lose directionality. The loss of the directionality of the two types of hydrogen bonds supports thin films as being amorphous.

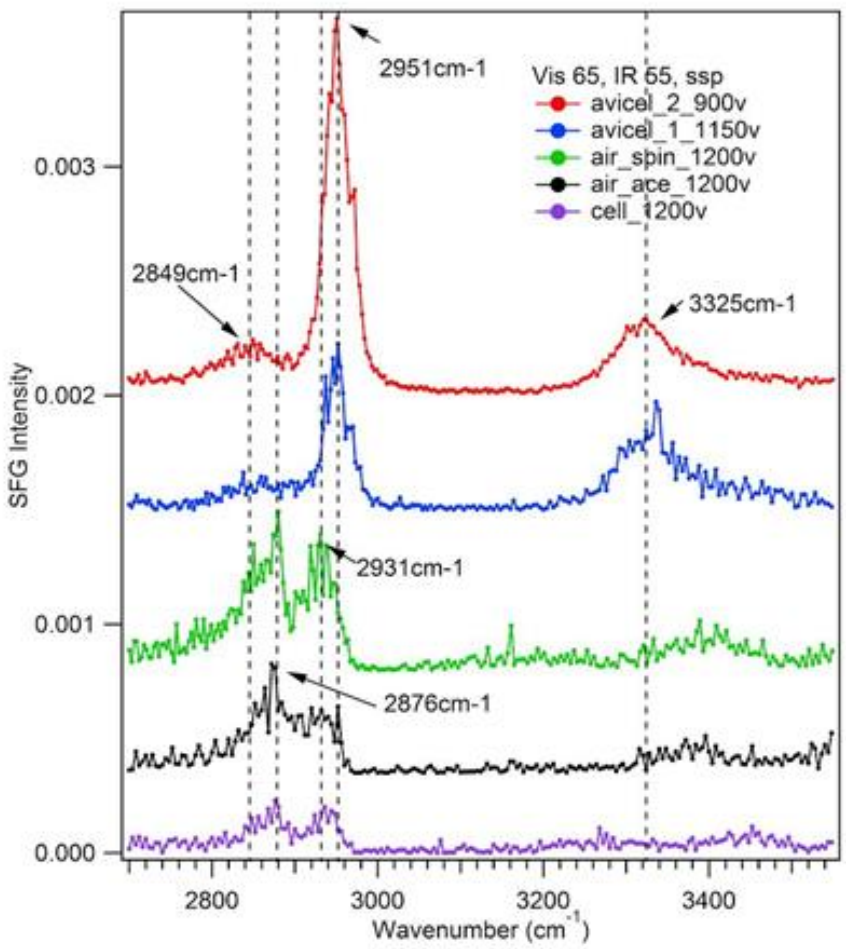

Figure 2.5 HR-SFG-VS spectra showing disappearance of peaks at 3325 cm-1 and 2951 cm-1, indicating O-H and C-H hydrogen bonds losing directionality, as a result of amorphous film formation.

2.3.2 Film Stability in Hydrochloric Acid Solution

A hydrochloric acid solution (pH=2) was made from concentrated HCl solution purchased from Sigma Aldrich. The cellulose thin film (29 nm) prepared from 1% cellulose solution at 1000 rpm was soaked in the HCl solution for 60 minutes. The film roughened from RMS 0.64 nm to 1.48 nm as measured by AFM and maintained integrity as assessed visually shown in Figure 2.6.

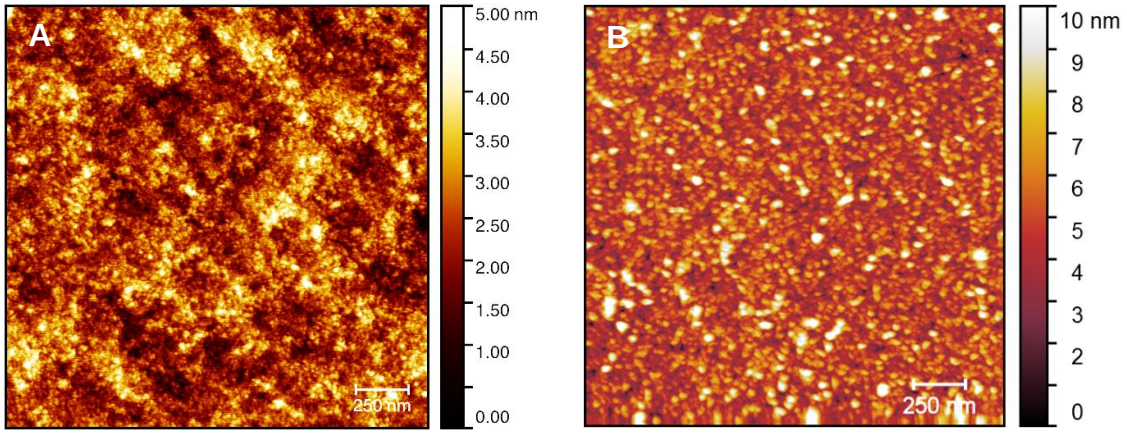

Figure 2.6 AFM of 1% cellulose films spincoated at 1000rpm (29 nm), (A) original cellulose thin film (RMS 0.64 nm); (B) cellulose thin film (RMS 1.4 nm) in hydrochloric acid solution (PH=2) for an hour.

2.3.3 Film Stability in Alkali Solutions

The cellulose thin films appear grayish and transparent in optical microscopy images as the films soaked in alkali solutions. Due to the smoothness of the films, it is difficult to distinguish whether there is film remaining on the silicon wafer. A scratch is helpful to observe if there is film left after soaking in alkali solution.

A cellulose thin film (29 nm) was spincoated at 1000 rpm from 1% cellulose solution and Figure 2.7 A shows a scratch on the it with obvious film residue along the scratch. Figure 2.7 B shows a hard scratch on silicon wafer for comparison (weak scratches on silicon wafer are difficult to observe by optical microscopy).

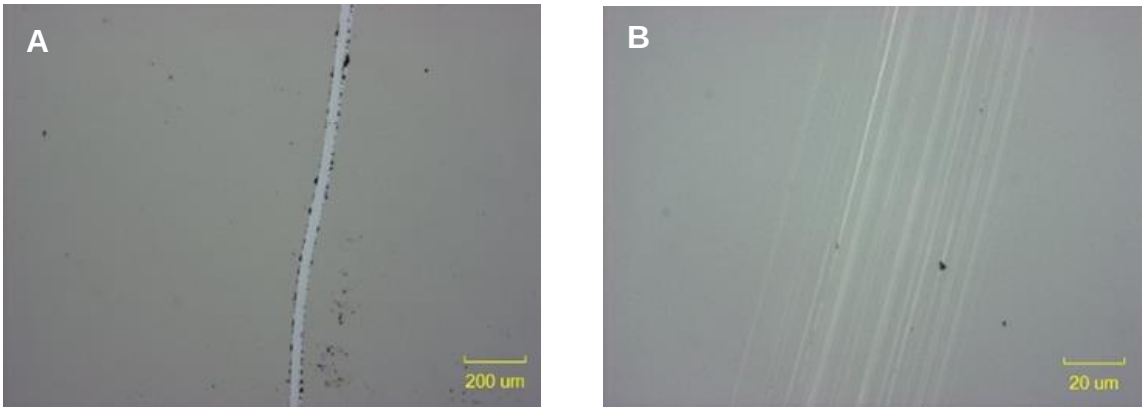

Figure 2.7 Optical images of scratches on (A) original cellulose thin films (29nm); (B) silicon wafer.

2.3.3.1 Sodium Hydroxide Solution

1 wt% and 5 wt% NaOH solutions in deionized (DI) water were made using reagent grade chemicals purchased from Sigma Aldrich without further purification.

The cellulose films made from 1% cellulose solution at 1000 rpm (29 nm) were soaked in 1 wt% and 5 wt% NaOH solutions respectively for an hour at room temperature. After soaking, there was still film left on the substrates as shown in Figure 2.8. The film was partially submerged in the solutions and the boundary between the original cellulose film and etched film can be observed due to the thickness difference. A stronger etching solution of 7 wt% NaOH/12 wt% urea/81 wt% DI water dissolution system was utilized to measure the etching rate.

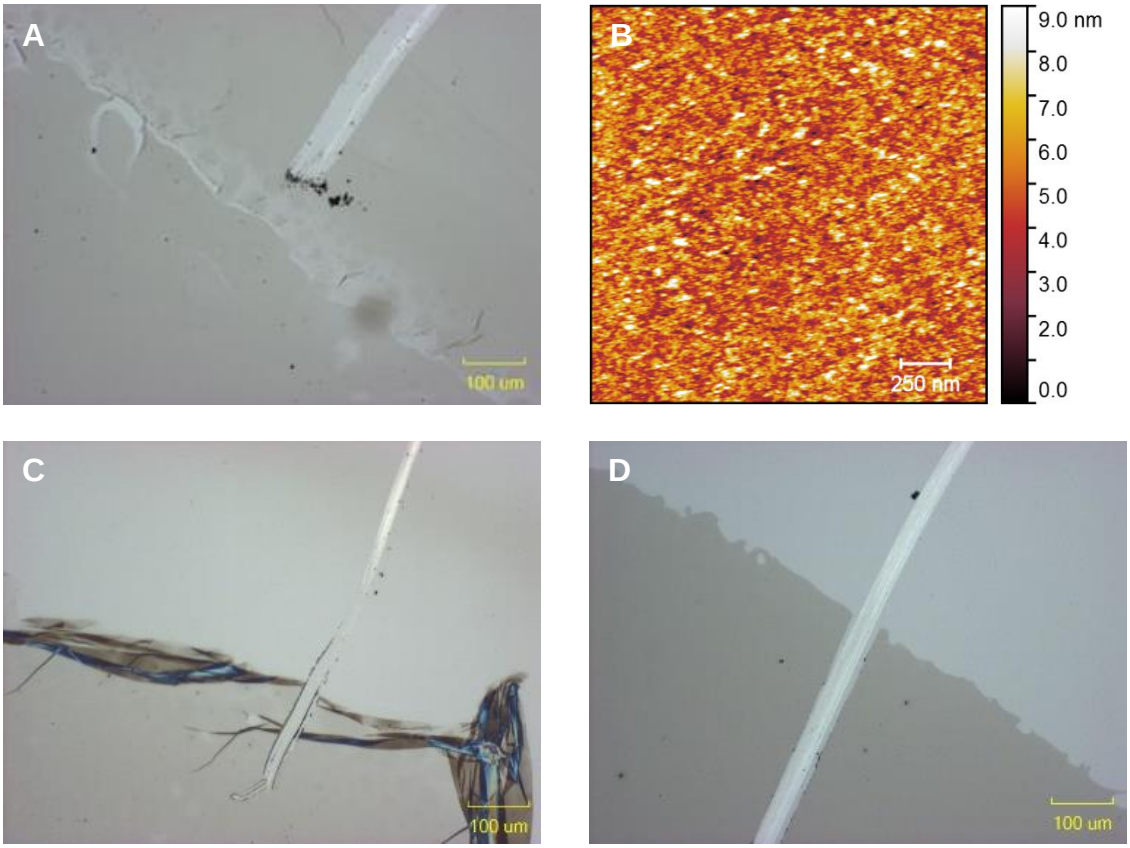

Figure 2.8 Optical images and AFM of cellulose films (A) cellulose thin film in 1 wt% NaOH solution at room temperature for 1 hour; (B) smooth cellulose film after 1 hour in 1 wt% NaOH solution at room temperature; (C) cellulose thin film in 5 wt% NaOH solution at room temperature for 1 hour; (D) cellulose thin film in 5 wt% NaOH solution at room temperature for 1 hour.

2.3.3.2 Sodium Hydroxide/ Urea Solution

Analytical grade NaOH and urea were used without further purification. As indicated in the literature [56-58], the most common concentration of alkali solution used to dissolve cellulose is 7 wt% NaOH/12 wt% urea/81 wt% DI water or 6 wt% NaOH/4 wt% urea/90 wt% DI water. The dissolution is temperature dependent and a lower temperature facilitates dissolution of cellulose. In this research, 7% NaOH/12% urea system at 273K was chosen for the ~50 nm cellulose thin films (1% cellulose solution spincoated at 600 rpm) etching experiments as a function of soaking time as shown in Figure 2.9.

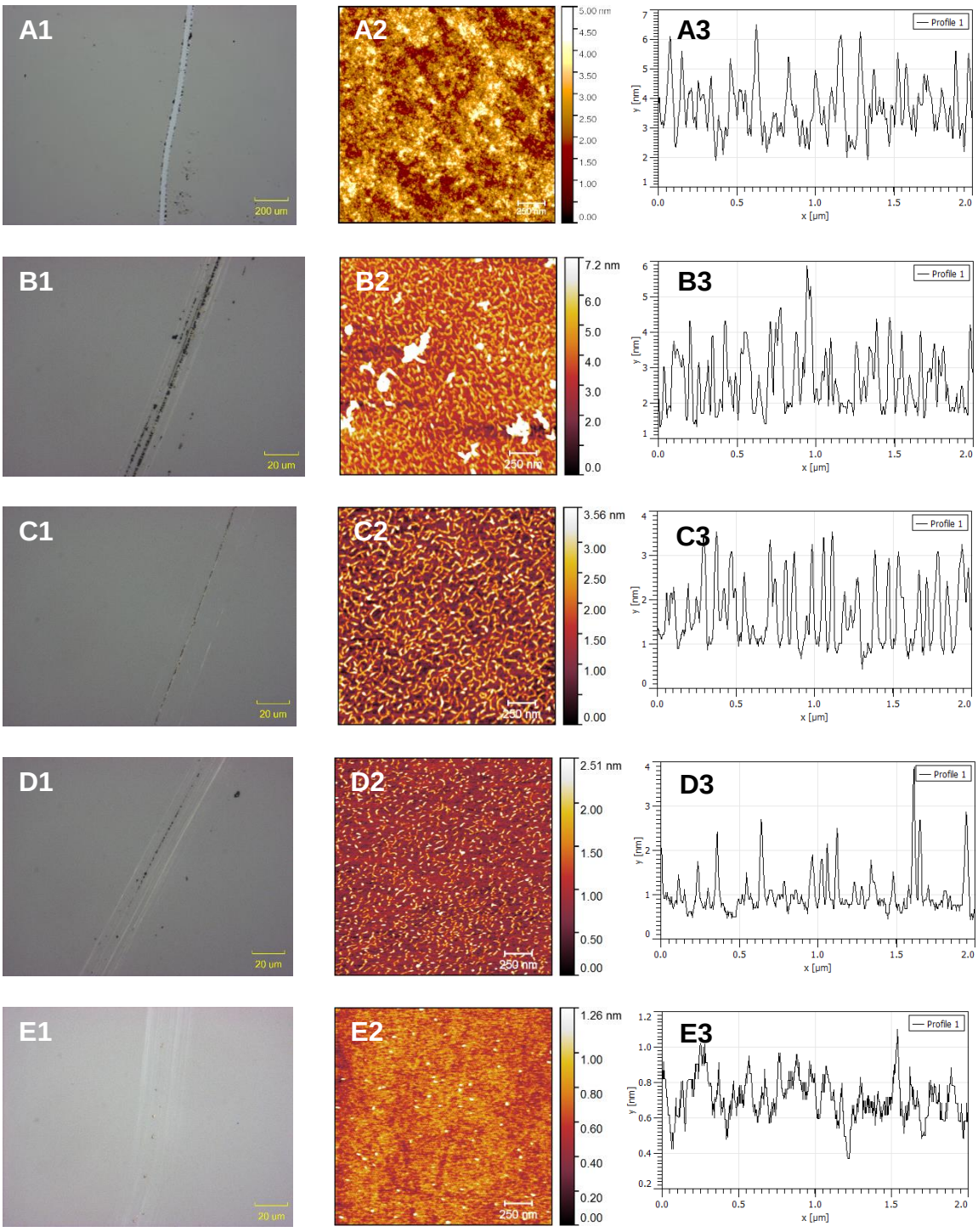
A1
200 um
A2
250 nm
5.00 nm
4.50
4.00
3.50
3.00
2.50
2.00
1.50
1.00
0.00
A3
Profile 1
y [nm]
x [µm]
B1
20 um
B2
250 nm
7.2 nm
6.0
5.0
4.0
3.0
2.0
0.0
B3
Profile 1
y [nm]
x [µm]
C1
20 um
C2
250 nm
3.56 nm
3.00
2.50
2.00
1.50
1.00
0.00
C3
Profile 1
y [nm]
x [µm]
D1
20 um
D2
250 nm
2.51 nm
2.00
1.50
1.00
0.50
0.00
D3
Profile 1
y [nm]
x [µm]
E1
20 um
E2
250 nm
1.26 nm
1.00
0.80
0.60
0.40
0.20
0.00
E3
Profile 1
y [nm]
x [µm]

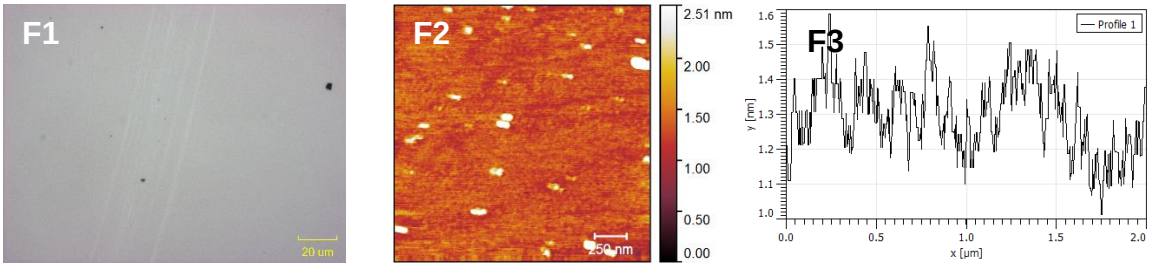

Figure 2.9 Optical images, AFM and height profile images of cellulose films in 7% NaOH/12% urea system at 273K for (A) original cellulose film; (B) 1 minute; (C) 5 minutes; (D) 15 minutes; (E) 30 minutes and (F) 60 minutes.

The RMS roughness and thickness of the amorphous cellulose thin films as a function of NaOH/urea etching are collected in Table 2.1 and plotted in Figure. 2.10.

Table 2.1 RMS roughness and thickness change during the NaOH/urea etching process.

	(A) Original	(B) 1 min	(C) 5 min	(D) 15 min	(E) 30 min	(F) 60 min
RMS (nm)	0.96	0.89	0.75	0.45	0.14	0.11
t (nm)	50±5	32±3	20±2	13±2	7±2	3±2

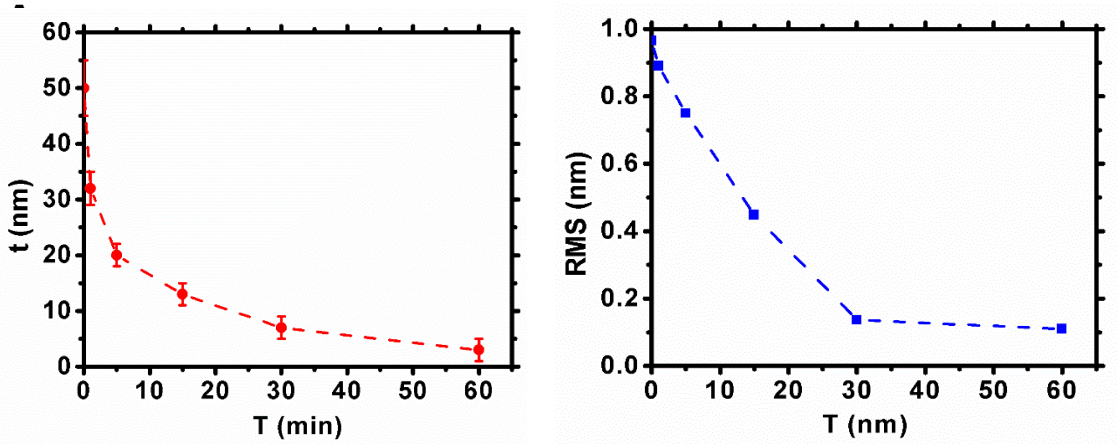

Figure 2.10 (A) Thickness and (B) RMS roughness of cellulose thin films while soaking in 7% NaOH/12% urea solution.

2.3.4 Film Stability in Hot Water

A cellulose thin film (29 nm) was prepared from 1% cellulose solution at 1000 rpm. DI water was heated to 363K and the film was soaked for 60 minutes. The film maintained integrity with RMS roughness increasing from 0.96 nm to 1.24 nm as shown in Figure 2.11.

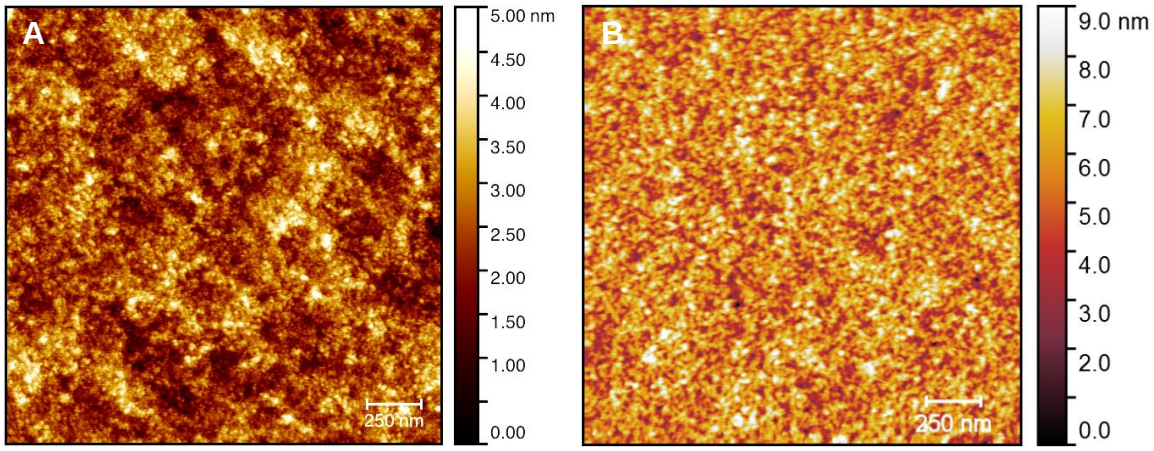

Figure 2.11 AFM of (A) original cellulose film (29nm); (B) cellulose thin film in hot water at 363K for 60 minutes.

2.3.5 Film Stability in Organic Solvents (DMSO, Acetone, Ethanol)

Cellulose thin films (29 nm) prepared from 1% cellulose solution at 1000 rpm were exposed to ethanol and acetone respectively for up to 5 hours before the surface started to show some short rupture lines along the film.

Pure cellulose cannot dissolve in DMSO without the addition of IL. This shows the film is quite stable in DMSO.

2.3.6 Thin Film with Controllable Thickness

2.3.6.1 Film Structure Change as a Function of Processing

By preparing cellulose molecular solutions of different concentrations and changing the spin speed, cellulose thin films with controllable thicknesses were obtained. As the thickness increased, the cycle process of vacuum, acetone soaking, ethanol rinse and blow dry was not capable of fully removing the IL. One wash cycle for films around 50 nm in thickness (1 wt% cellulose films spincoated at 600 rpm) was found to be sufficient to remove the EMIM Ac by XRR as shown in Figure 2.12. The sample washed one time had the same XRR curve as the sample washed two times.

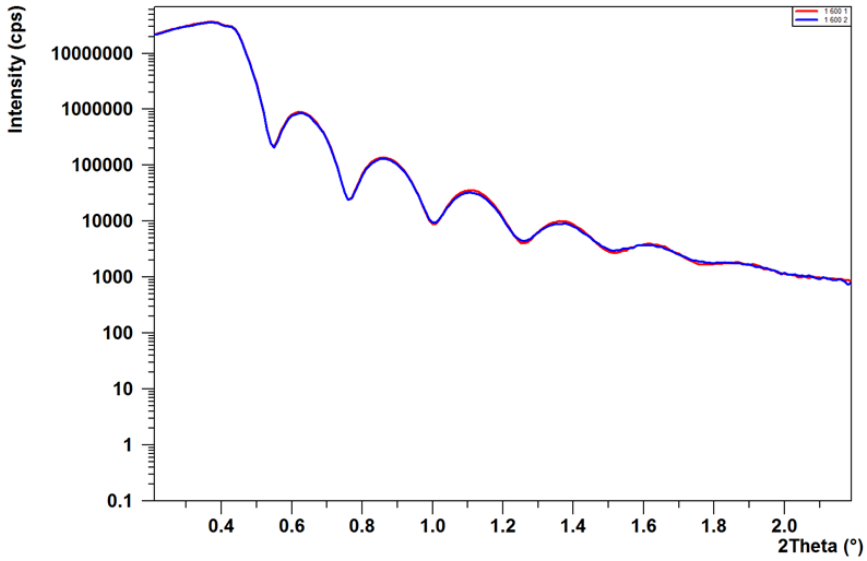

Figure 2.12 XRR of 1% cellulose films at 600 rpm with one time wash and two times wash.

The X'Pert Pro MRD XRR instrument, had the best resolution for films less than 100 nm, a 90 nm film around was chosen to test whether repeating the cleaning cycle could fully remove the IL. The cycle was repeated three times and then the film was soaked in 7 wt% NaOH/12 wt% urea solution as an additional test to establish whether

the EMIM Ac was fully removed. Figure 2.13 shows the AFM images indicating the morphological changes during the process. The observation of worm-like structures after soaking in the NaOH/urea solution changes from 49.0% to 57.9% and eventually to 68.3%, which helped to elucidate the IL removal. The existence of IL accelerates the etching process. As the area of worm-like structure became dense, there was more film left on the silicon wafer and the film showed stronger resistance to etching by the alkali solution.

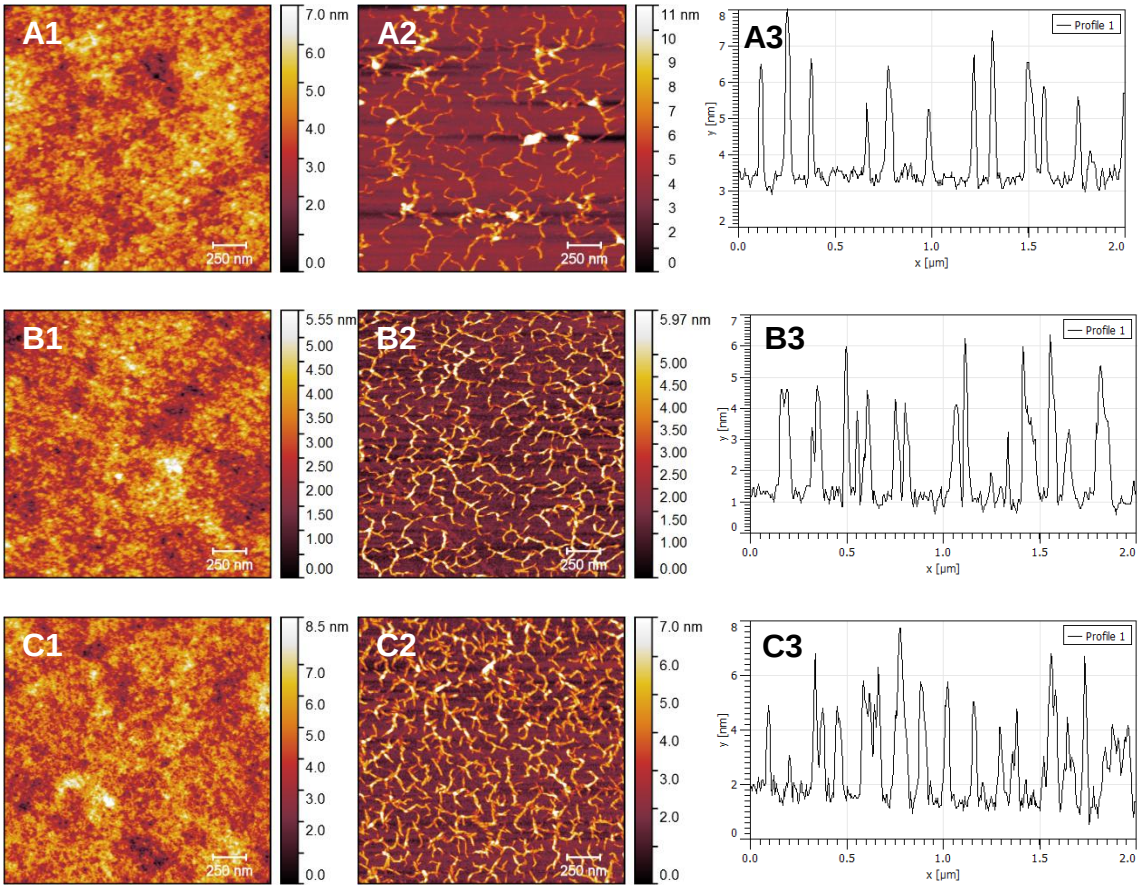

Figure 2.13 AFM and height profile of cellulose films structure changes as processing (A1) one time wash cellulose thin film, (A2) one time wash cellulose film soaked in NaOH/urea solution for 5 minutes, (A3) height profile of one time wash cellulose thin film; (B1) two times wash cellulose thin film, (B2) two times wash cellulose film soaked in NaOH/urea solution for 5 minutes, (B3) height profile of two times wash cellulose thin film; (C1) three times wash cellulose thin film, (C2) three times wash cellulose film soaked in NaOH/urea solution for 5 minutes, (C3) height profile of three times wash cellulose thin film.

2.3.6.2 Film Thickness Change as a Function of Processing

The thickness of the cellulose thin film can be controlled by changing the spin speed and concentration of the cellulose molecular solutions. Films less than 10 nm thick were obtained from 0.5 wt% cellulose solution at 3000rpm spin speed. At higher concentrations, the viscosity was too high for spincoating. The solution and spinner were heated to 333K (for 2% cellulose solution) and 363K (for 3% and 4% cellulose solutions) to reduce the viscosity. 4 wt% cellulose solution was used to produce the thickest film. As Figure 2.14 shows, the RMS roughness among all the films with different thicknesses was controlled below 2 nm. Specific parameter information is provided in Table 2.2.

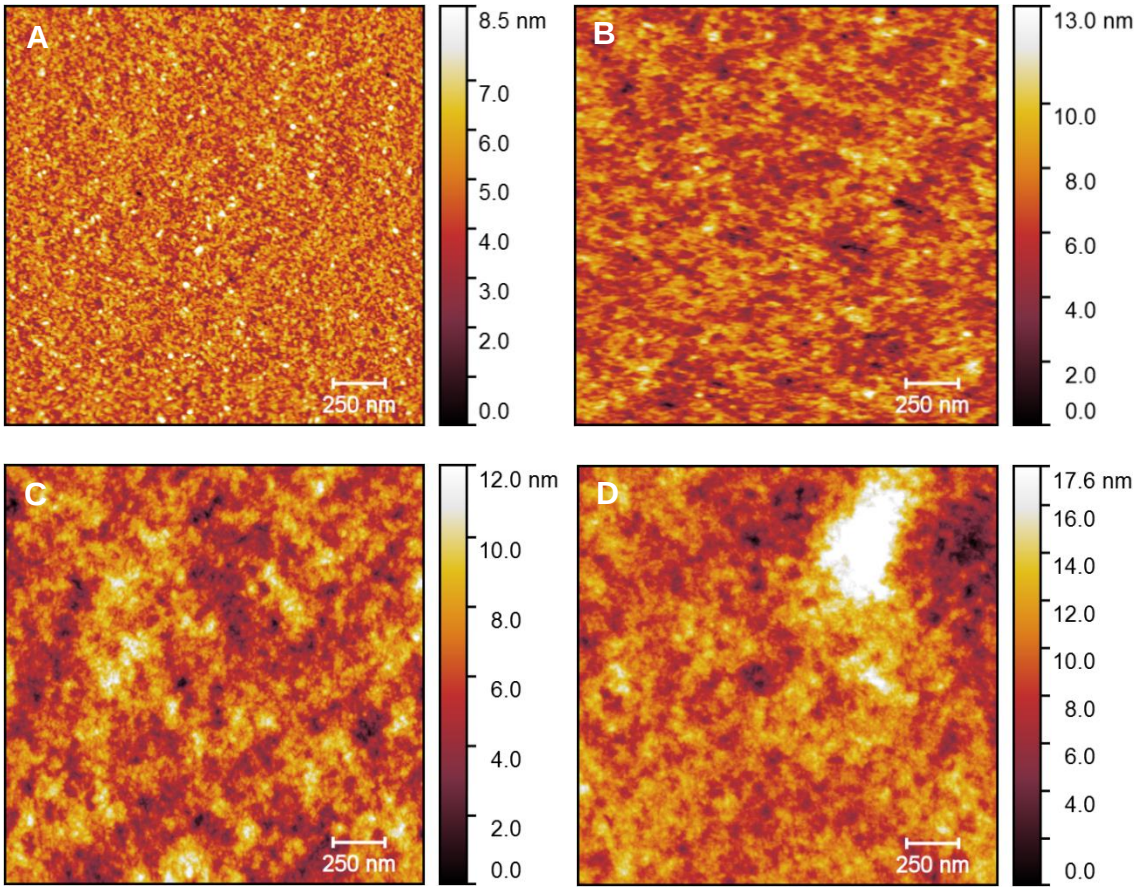

Figure 2.14 AFM of cellulose films with different thickness as processing (A) 0.6% cellulose solution at 3000rpm, RT; (B) 2% cellulose solution at 1000rpm, 333K; (C) 3% cellulose solution at 1000rpm, 363K; (D) 4% cellulose solution at 1000rpm, 363K.

Table 2.2 Roughness and thickness of cellulose thin films as a function of processing

Film parameter	(A) 0.6%, 3k rpm, RT	(B) 2%, 1k rpm, 333K	(C) 3%, 1k rpm, 363K	(D) 4%, 1k rpm, 363K
RMS (nm)	1.01	1.53	1.67	1.73
Thickness (nm)	8	120	325	336

XRR measurements from the glassy cellulose thin films with increasing thickness from ~ 8 nm to ~ 90 nm are shown in Figure 2.15 with vertically shifted curves for a better comparison. All curves of different thickness showed oscillations which indicates the films all flat over the full range of thicknesses. Utilizing Reflpak [59] analysis software from NIST Center for Neutron Research, a model was built to interpret the XRR data as shown in Figure 2.16 A for the sample labeled 29 nm in Figure 2.15. Figure 2.16 B shows the density and void volume ratio change as the function of the film thickness. The fitting results for all the data in Figure 2.15 is based on a one-layer model and the parameters are given in Table 2.3. The electron number density and mass density of the cellulose thin films were consistent with that of bulk amorphous cellulose $\rho = 1.5$ g/cm^3. As the DMSO and EMIM Ac were removed from the thin film, small voids were created which resulted in a decrease of the cellulose thin film density compared with bulk amorphous cellulose density. This was used to calculate the void volume ratio. According to Figure 2.16 B, there is a threshold of film thickness around 20 nm to 30 nm. Below the threshold, the film showed a relatively higher void percentage and lower void percentage were observed for this films above the threshold thickness. The two main reasons may be (1) during the spincoating process, a mixture of acetone and toluene were used to remove

part of the DMSO and EMIM Ac, but for thinner films (<20 nm), the process could be too fast to allow the cellulose chains to relax, (2) the top and bottom layer at the Si and air interface is a larger fraction of the film volume ratio than for thicker films. A three-layer model of the cellulose thin film electron number density profile is shown in Figure 2.17 using the same sample as used for the one-layer model and the fitting results are shown in Table 2.4. The top layer thicknesses of all films were held constant at ~2 nm and the cellulose bulk layer and the lower layer thickness was found to obey a linear relationship with the total thickness.

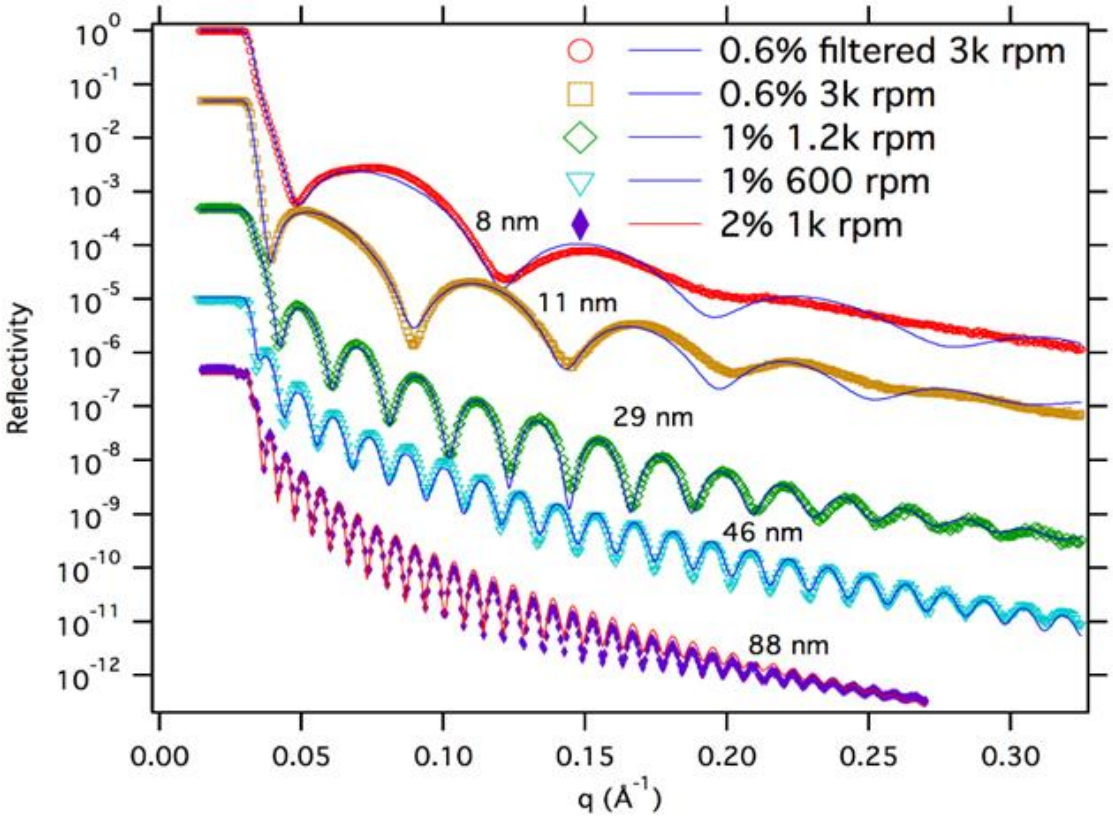

Figure 2.15 Vertically shifted X-ray reflectivity (XRR) curves for glassy cellulose thin films Oscillations indicate the flat surface with limited roughness.

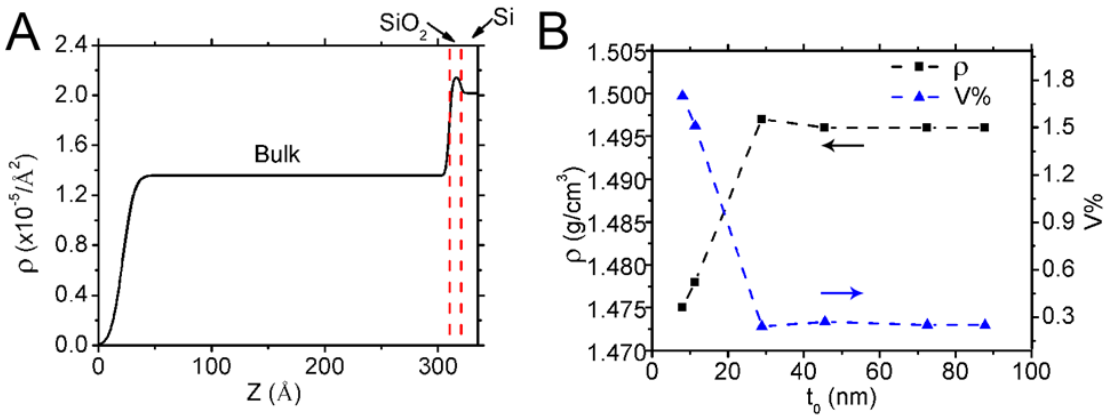

Figure 2.16 (A) one-layer model of the cellulose thin film electron number density profile labeled as 29 nm in Figure 2.15; (B) density and void volume ratio trend of cellulose thin films changing with the film thickness.

Table 2.3 One-layer XRR fitting results for cellulose glass thin films

Sample name	XRR thickness (nm)	RMS roughness (nm)	Electron number density ($\times 10^{-5}$ Å^{-2})	Mass density (g/cm^3)	%Vol of void
0.6%, 3k rpm	8.0	0.7	1.3333±0.0000	1.475	1.70
0.6%, 2k rpm	11.3	1.3	1.3357	1.478	1.51
1%, 1.2k rpm	28.9	1.9	1.3529	1.497	0.24
1%, 0.6k rpm	45.5	0.9	1.3524	1.496	0.27
2%, 1.8k rpm	72.5	0.8	1.3527	1.496	0.25
2%, 1k rpm	87.7	2.6	1.3527	1.496	0.25

(Error of electron number density of all XRR data is ~ ±0.00003)

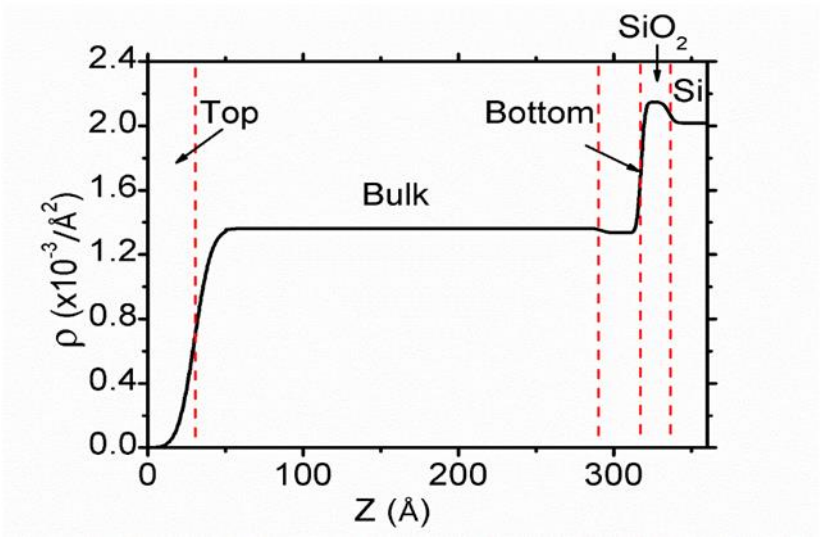

Figure 2.17 Three-layer model of the cellulose thin film electron number density profile labeled as 29 nm in Figure 2.15.

Table 2.4 Three-layer XRR fitting results for cellulose glass thin films

	0.6% 3k rpm	0.6% 2k rpm	1% 1.2k rpm	1% 0.6k rpm	2% 1.8k rpm	2% 1k rpm
XRR thickness (nm)	8.2	11.2	28.7	45.5	72.4	87.6
Electron number density (Top) ($\times10^{-5}$ Å^{-2})	1.3400	1.3415	1.3403	1.3423	1.3414	1.3365
Mass density (Top) (g/cm^3)	1.482	1.484	1.483	1.485	1.484	1.478
XRR Top thickness (nm)	1.9	1.9	2.0	2.3	2.5	2.5
Electron number density (Bulk) ($\times10^{-5}$ Å^{-2})	1.3559	1.3559	1.3557	1.3544	1.3549	1.3545
Mass density (Bulk) (g/cm^3)	1.499	1.499	1.499	1.498	1.498	1.498
XRR Bulk thickness (nm)	4.4	7.3	24.2	39.6	65.5	79.6
Electron number density (bottom) ($\times10^{-5}$ Å^{-2})	1.3252	1.3276	1.3284	1.3262	1.3255	1.3305
Mass density (Bottom) (g/cm^3)	1.466	1.468	1.470	1.467	1.466	1.472

XRR Bottom thickness (nm)	1.8	2.0	2.5	3.7	4.4	5.6

2.4 Conclusions

An acetone and toluene wash mixture was chosen to remove DMSO and EMIM Ac during the spincoating process. This wash mixture can help create a stable gel-like layer on top of the cellulose thin film during spincoating. The slow removal process for DMSO and EMIM Ac produces a flat surface by minimizing the stress produced due to the removal of the DMSO and EMIM Ac. Although acetone and toluene can both dissolve DMSO, the largest amount of DMSO is removed under vacuum after spincoating. Acetone has a low solubility of EMIM Ac and faster evaporation than toluene. Toluene does not mix with EMIM Ac at all. These two factors resulted in the limited removal of DMSO and EMIM Ac, during the spincoating/wash process which caused a reflow of EMIM Ac into the film resulting in a smooth film surface. EMIM Ac has low solubility in acetone, but using fresh acetone to remove EMIM Ac was proved to be helpful by XRD. Rein and coworkers found that EMIM cations and Ac anions recombine in acetone leading to a concentration gradient which helps drive the EMIM Ac out of the cellulose films [60]. The EMIM Ac collected in the acetone could be recycled and reused.

XRR, XRD, HR-SFG-VS and AFM all support that the thin cellulose films spincoated from IL/DMSO and washed with acetone and toluene are amorphous. Films ranging from less than 10 nm to more than 100 nm can be produced without any crystalline structure by adjusting the concentration of cellulose solutions and the spin speed. As the film thickness increases, more times of soaking in acetone can be repeated to remove the EMIM Ac as thoroughly as possible. The amorphous cellulose thin film

exhibited stability in hot water, acid solution, low concentration base solution and most organic solvents except oxidizing acid solution and strong base solution [34].

Chapter 3: Blend Thin Film of Cellulose and Polyacrylonitrile

3.1 Introduction

As explained in Chapter 1, a goal is to formulate a cellulose composite with novel properties (better resistance of etching) and expand the applications of cellulose products [61-63].

Polyacrylonitrile (PAN) possesses excellent mechanical properties, chemical stability and non-toxicity that make it a great material for fibers, membranes and electronics [42,45]. PAN hollow fiber membranes were prepared from IL and DMSO system for osmosis application and phase separation of the polymer solutions was found because of water. [42] Composite cellulose/polyacrylonitrile films was produced by Bochek and coworkers from the IL/dimethylformamide (DMF) solution. A mixed network of weaker intermolecular hydrogen bonds was formed in the blend solutions compared to that in pure cellulose/IL/DMSO solutions. It provided the information that when there were more than 50% polyacrylonitrile in the films, the two materials will not be compatible with each other. [49] These conclusions helped to design and understand cellulose and PAN blend in IL/DMSO solution system.

In this chapter, thin film blends made of cellulose and polyacrylonitrile (PAN) was prepared and their stability in harsh conditions were examined. The nanocomposite showed better chemical resistance than pure cellulose and pure PAN according to XRR and AFM data.

3.2 Experimental

3.2.1 Blend Thin Film Preparation

1% cellulose solution was prepared as discussed in Chapter 2. PAN solutions were prepared by dissolving 1% PAN purchased from Scientific Polymer Products, Inc. in a mixture of 3% EMIM Ac and 96% DMSO. The clear solutions of both materials were mixed at a ratio of 1: 1.

The preparation method of the blend thin films was the same as preparing cellulose thin films. A glass bell jar was filled with N_2 after the substrate was put on the spinner holder. 1000 rpm spin speed was used initially for 5 minutes followed by 100 rpm for 30 seconds. During this second time period, a mixture of 1:1 weight ratio of anhydrous acetone and toluene was poured continuously and carefully onto the blend films to extract part of DMSO and EMIM Ac. The last step was washing the film with anhydrous acetone for 20 seconds and spin dry for 40s. The vitrified films were then put into a vacuum oven at 333K to remove the rest of the DMSO and soaked in fresh acetone for 3 times (each time lasted 15 minutes) to remove remaining EMIM Ac. The film preparation was finished by rinsing with ethanol and then blow dry with N_2.

3.3 Results and Discussion

3.3.1 Morphology Characterization of Blend Films

AFM was used to characterize the surface morphology of the blend thin films and compared to that for pure PAN thin films. The concentration of both solutions was kept at 1% and the ratio of cellulose and PAN was 1:1 in the solution. The morphologies of the two thin films were similar with small roughness difference between them as shown in

Figure 3.1. The blend thin film showed no sign of phase separation with the roughness of 3.0 nm and the PAN thin film as 3.7 nm.

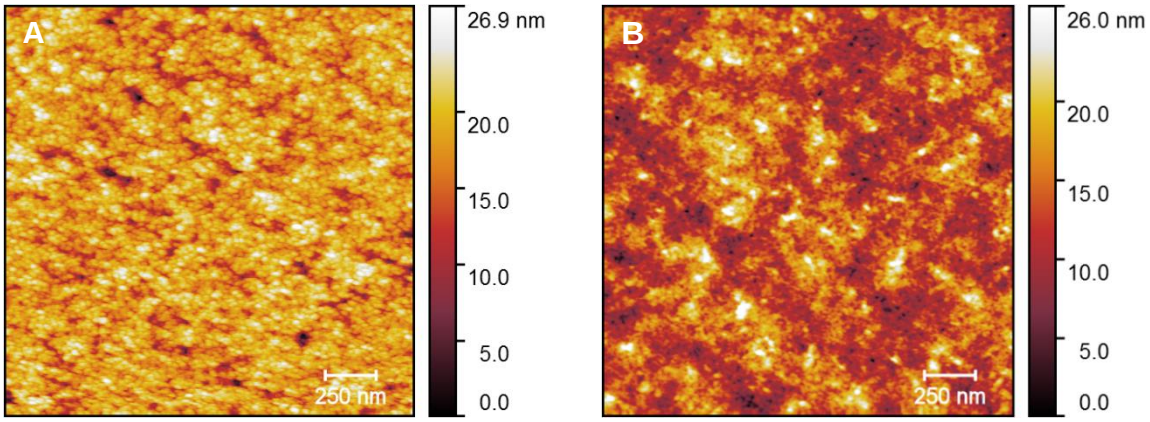

Figure 3.1 AFM of thin films made of (A) 1% cellulose: PAN=1: 1 solution (RMS 3.0 nm) and (B) 1% PAN solution at 1000rpm (RMS 3.7 nm).

3.3.2 Film Stability in Hydrochloric Acid Solution

0.1 M hydrochloric acid solution purchased from Sigma Aldrich was used to prepare the acidic solution (pH=2). The films were put in the HCl solution for 60 minutes at 298K. The film remained visually intact and had an RMS roughness increased from 3.0 nm to 4.2 nm as shown in Figure 3.2. The blend film stability in hydrochloric acid solution was similar as for pure cellulose thin film.

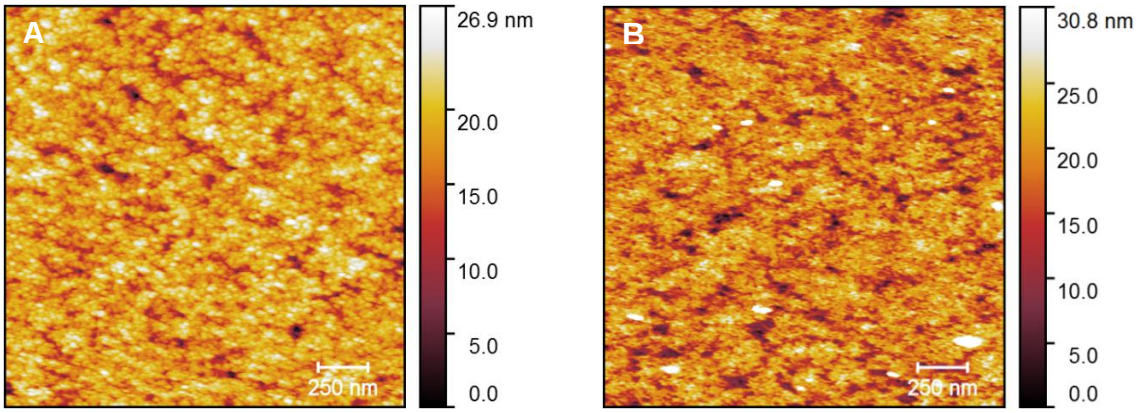

Figure 3.2 AFM of (A) cellulose: PAN=1: 1 thin film spincoated at 1000 rpm (RMS 3.0 nm); (B) the film soaked in HCl solution (PH= 2) for an hour (RMS 4.2 nm) at 298K.

3.3.3 Film Stability in Alkali Solutions

As described in Chapter 2, the stability test in alkali solutions is an important part of analyzing the thin film behavior, so as a comparison, the blend thin film of cellulose and PAN was soaked in alkali solutions and the resistance improved after 60 minutes soaking in NaOH/urea solution. The thicknesses remaining on the silicon wafer after soaking times of 1 minute, 5 minutes, 30 minutes and 60 minutes were all higher than those for pure cellulose films.

3.3.3.1 Sodium Hydroxide Solution

1% and 5% NaOH solutions were prepared and the cellulose: PAN = 1: 1 thin films were soaked at half depth at room temperature for one hour. The etched away part of the film was visually smooth compared to the original part as shown in Figure 3.3. Compared to the pure cellulose thin film etching, there was not much difference in the scratches. The blend thin films also showed stability in NaOH solutions.

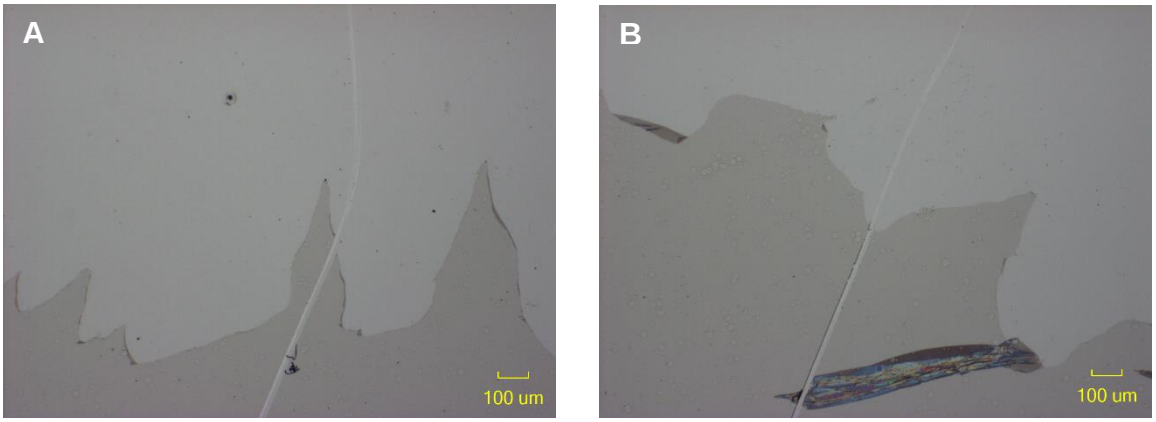

Figure 3.3 Optical images of cellulose: PAN =1: 1 thin film half soaked in (A) 1% NaOH solution; (B) 5% NaOH solution at room temperature for one hour.

3.3.3.2 Sodium Hydroxide/ Urea Solution

7% NaOH/12% urea/81% DI water (as in Chapter 2) was prepared to etch the blend thin film at 273K. Figure 3.4 and Figure 3.5 shows the morphology, thickness and roughness changes as the soaking time increased. PAN also dissolves rapidly in the NaOH/urea mixture due to the strong hydrolysis occurring. The blend thin films presented the same worm-like structure as the pure cellulose thin films soaked in 7% NaOH/12% urea solution and the blend thin film showed better resistance to etching after one hour soaking according to the thickness changes in Figure 3.5. A thicker film was left on the substrate than for pure cellulose thin films, which proves the stronger resistance of blend thin films. Both cellulose thin films and blend thin films were ~55nm. The thickness change of the blend thin films in Figure 3.5 A are slower than that of pure cellulose thin films in Figure 2.10 A. After 60 minutes soaking in NaOH /urea solutions, the AFM showed no pure cellulose thin film left in Figure 2.9 F2 while the blend thin films was found to keep a layer with 13 nm thickness with structure shown in Figure 3.4 E1.

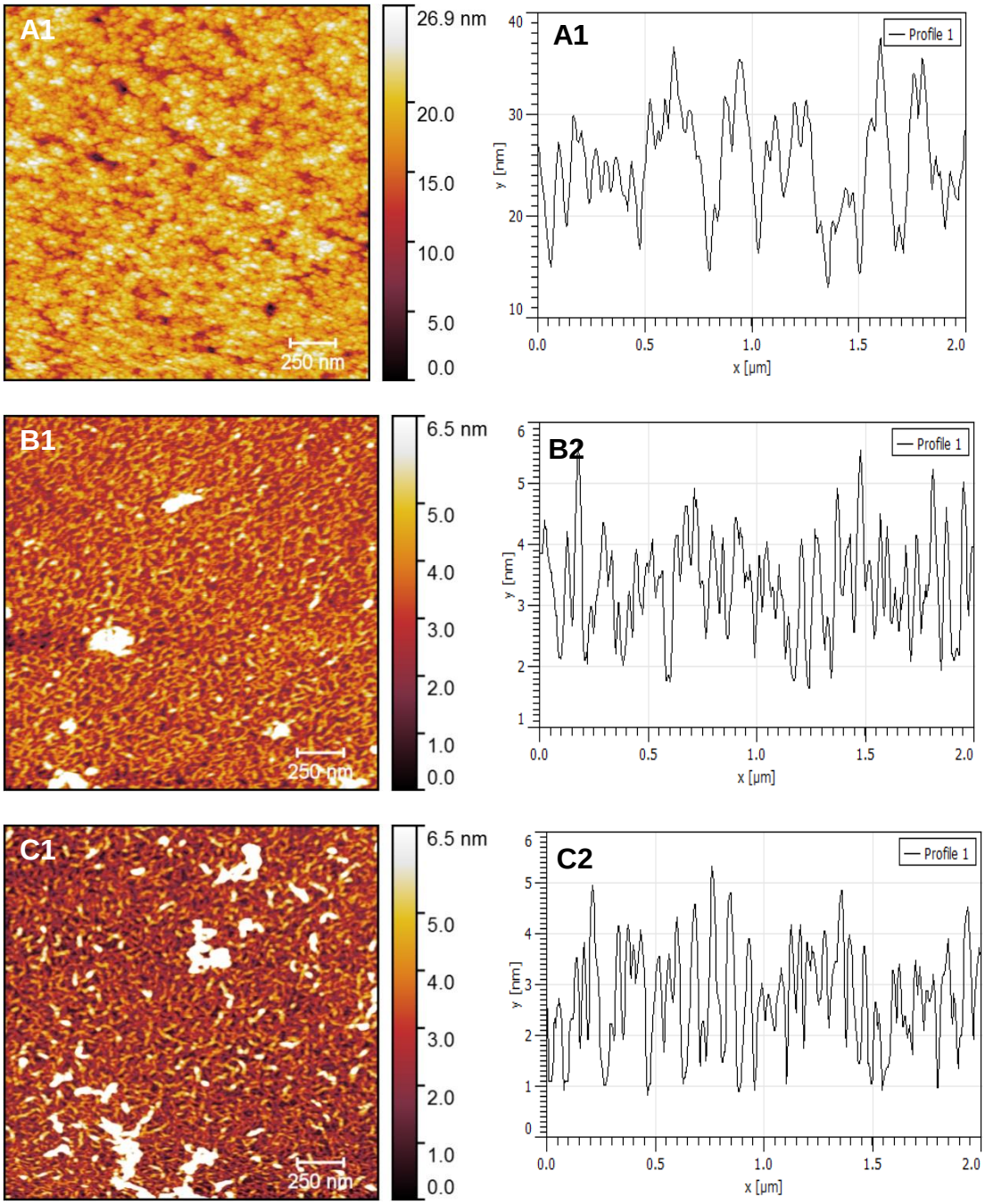
A1
26.9 nm
20.0
15.0
10.0
5.0
0.0
250 nm
A1
Profile 1
y [nm]
x [µm]
B1
6.5 nm
5.0
4.0
3.0
2.0
1.0
0.0
250 nm
B2
Profile 1
y [nm]
x [µm]
C1
6.5 nm
5.0
4.0
3.0
2.0
1.0
0.0
250 nm
C2
Profile 1
y [nm]
x [µm]

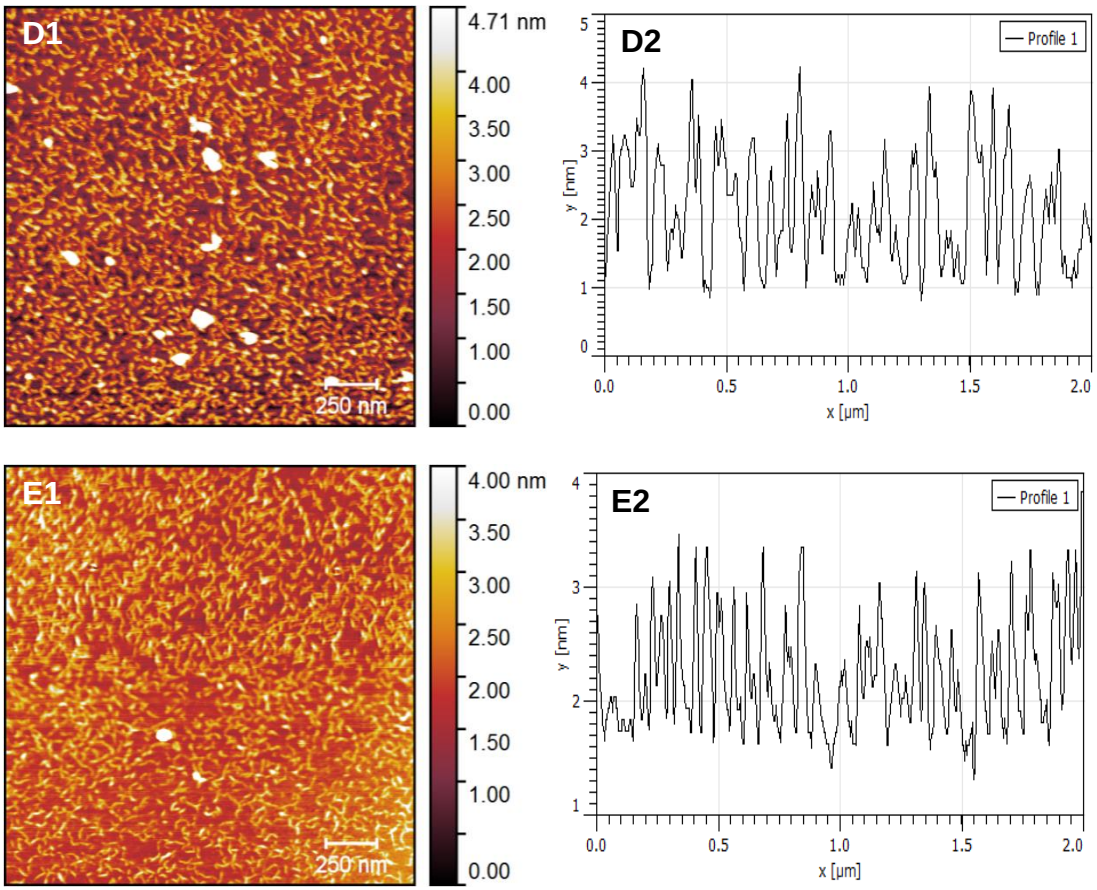

Figure 3.4 AFM and height profile images of cellulose: PAN=1: 1 films in 7% NaOH/12% urea system at 273K for (A) original blend thin film; (B) 1 minute; (C) 5 minutes; (D) 30 minutes and (E) 60 minutes.

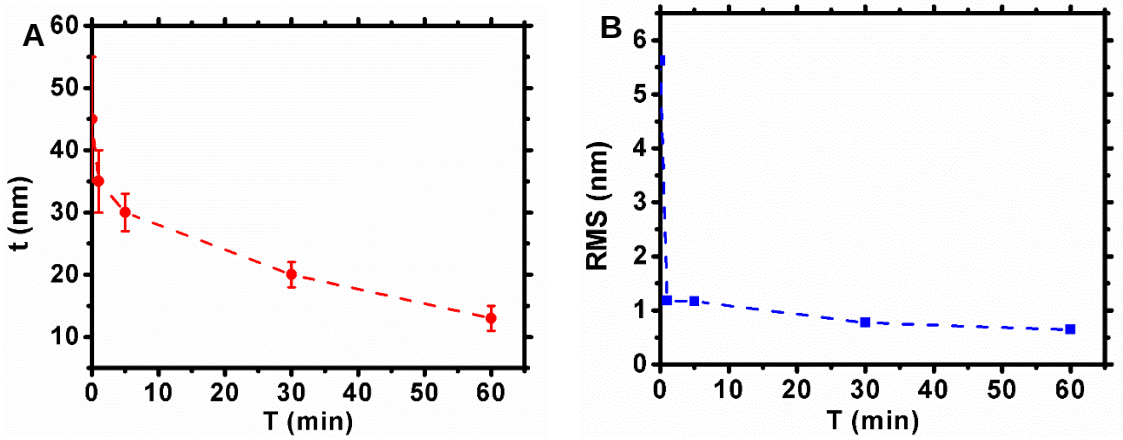

Figure 3.5 (A) Thickness; (B) RMS roughness of cellulose thin films while soaking in 7% NaOH/12% urea solution.

After the films were soaked in 7% NaOH/12% urea solution, the film was soaked in pure DMSO to remove the PAN, which would only leave the cellulose. AFM of these samples are shown in Figure 3.6 with thickness and roughness plotted in Figure 3.7. Visually there was no change of the blend thin films. Thin films with pores were observed by AFM showing the PAN distribution. The worm-like structure of all the films soaked in alkali solutions and DMSO got sparser than that of the films soaked in alkali solutions only.

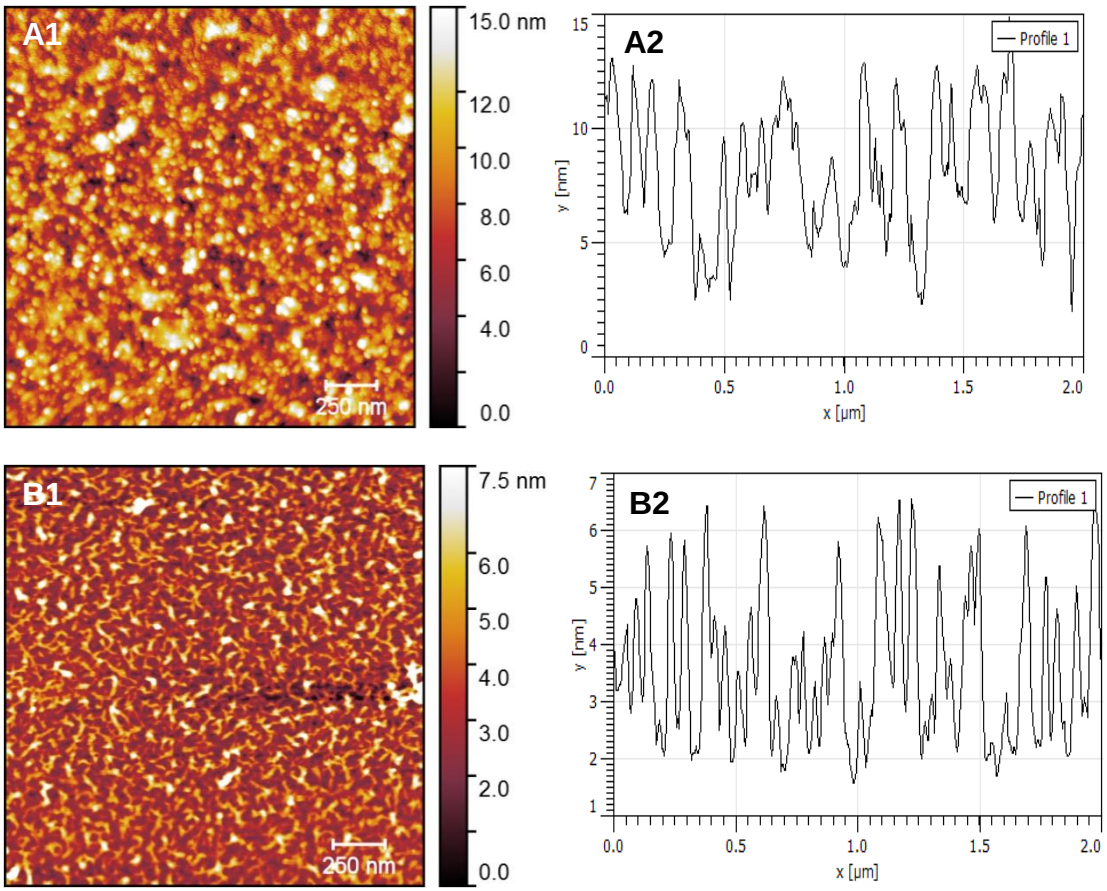

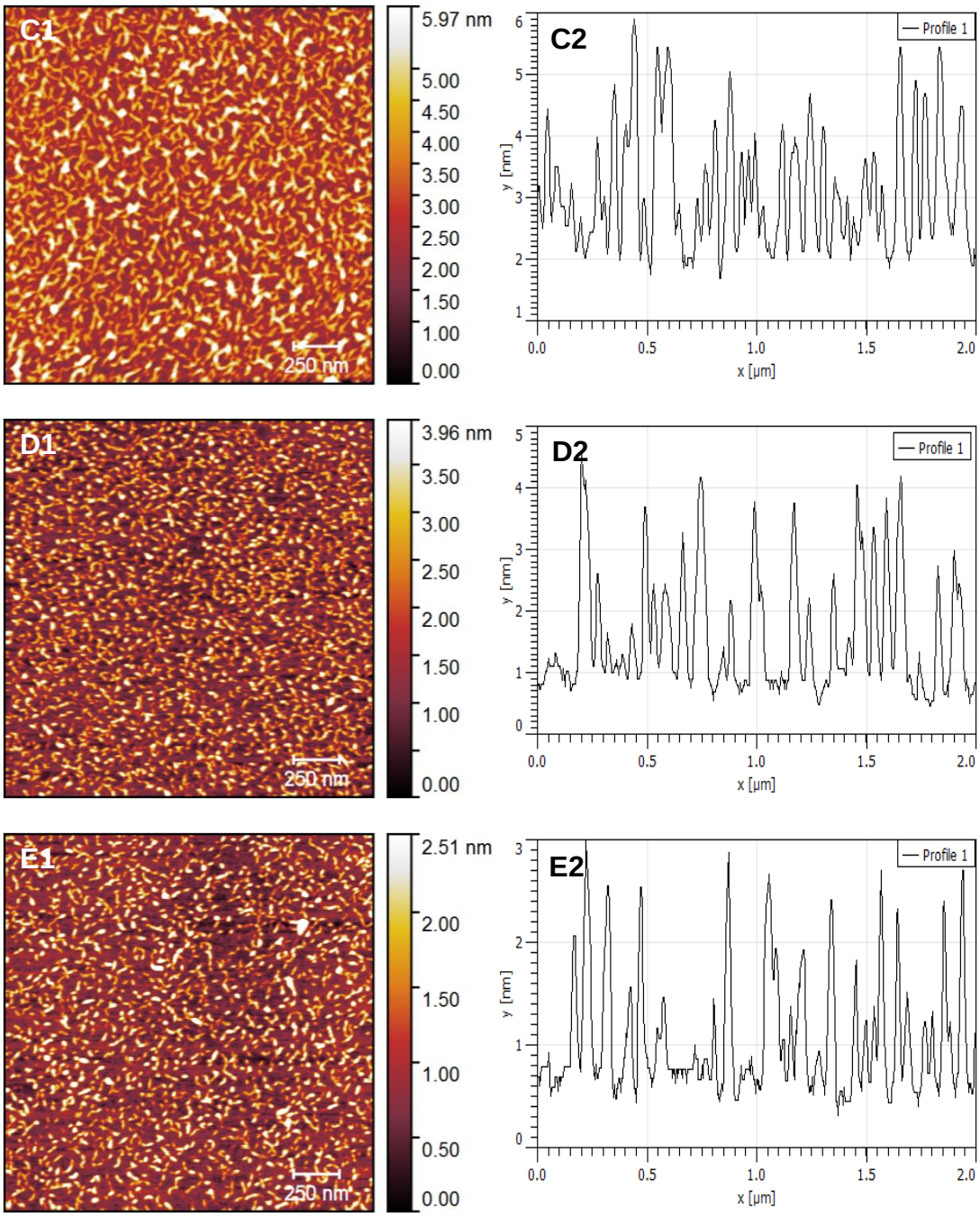

Figure 3.6 AFM and profile images of cellulose: PAN=1: 1 film in 7% NaOH/12% urea solution at 273K for (A) original thin film; (B) 1 minute; (C) 5 minutes; (D) 30 minutes and (E) 60 minutes and then all put in DMSO for 5 minutes to fully remove PAN which only left cellulose on the substrate.

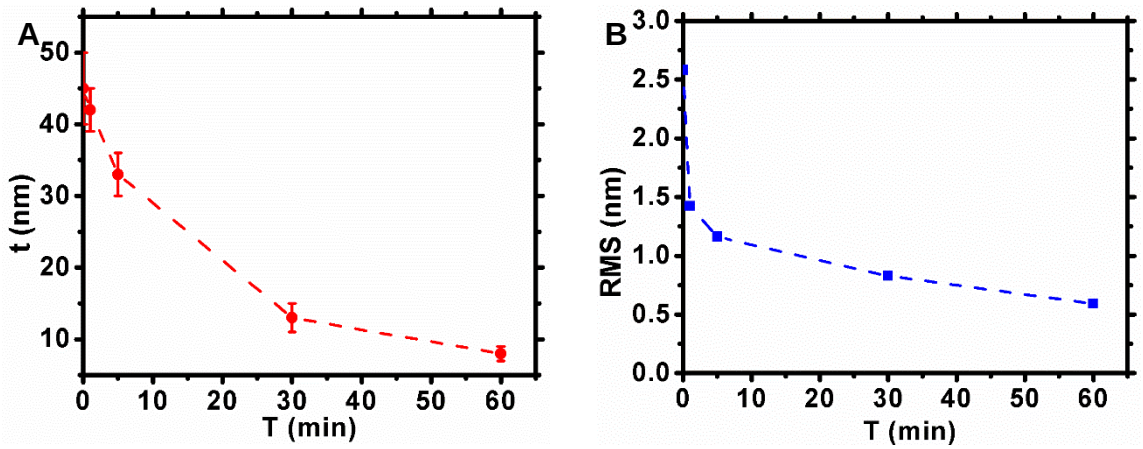

Figure 3.7 (A) Thickness and (B) RMS roughness of cellulose thin films after soaked in 7% NaOH/12% urea solution and in DMSO to completely remove PAN.

3.3.4 Film Stability in Hot water

The blend thin film of cellulose: PAN = 1: 1 was placed in the hot water for 10 minutes at 363K. The film roughened from 3.0 nm to 8.5 nm shown in Figure 3.8.

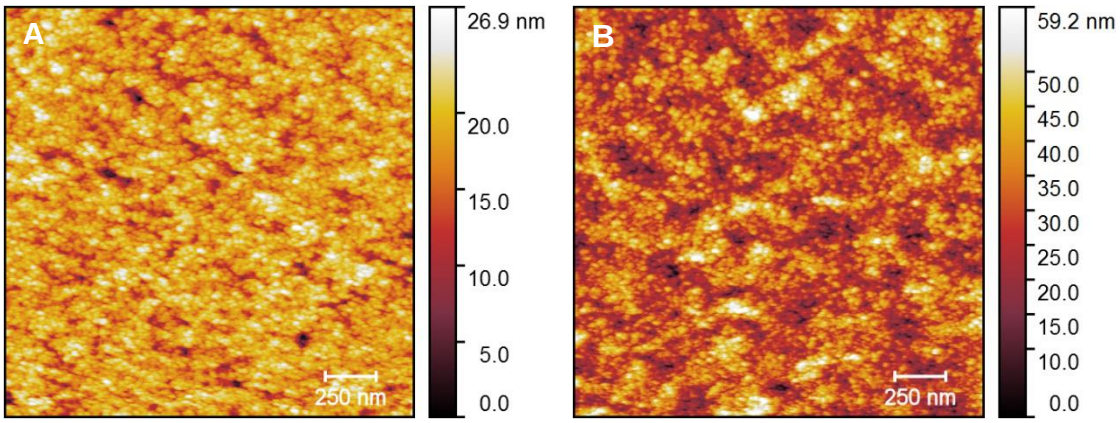

Figure 3.8 AFM of (A) cellulose: PAN=1: 1 film (RMS 3.0 nm); (B) PAN film (RMS 8.5 nm) in hot water at 363K for 10 minutes.

3.3.5 Film Stability in Organic Solvents (DMSO, Acetone, Ethanol)

The cellulose and PAN blend thin films were soaked in acetone and ethanol for 5 hours and showed no obvious changes.

However, when the blend thin film was soaked in DMSO, PAN easily dissolves as tested by 1% pure PAN thin film in DMSO for 5 minutes in Figure 3.9 A and B. This leaves only a cellulose nanoporous film on the silicon wafer shown as Figure 3.9 D. While this nanoporous thin film was still resistant to etching, it could possibly be used for filtration, membranes and packaging.

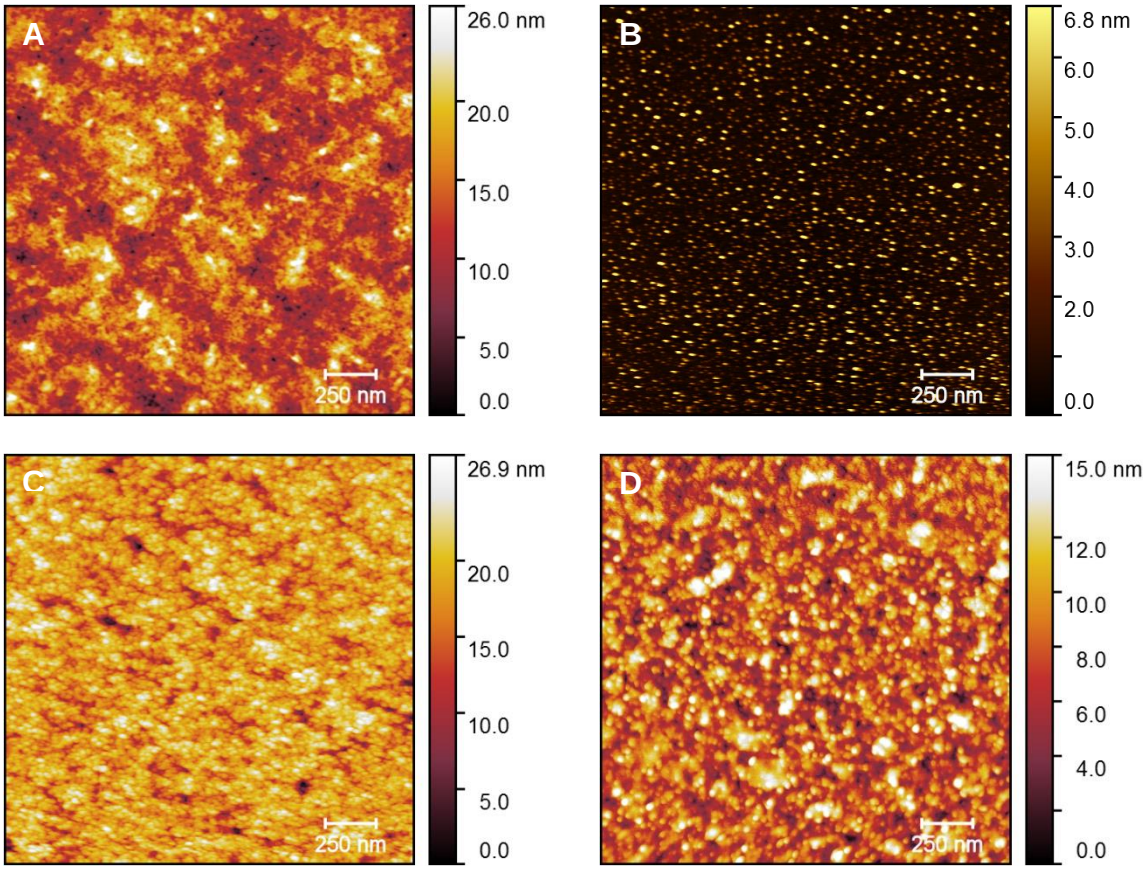

Figure 3.9 AFM images for (A) pure 1% PAN/ 3% EMIM Ac/ 96% DMSO thin film spincoated at 1000rpm; (B) pure 1% PAN thin film soaked in DMSO for 5 minutes; (C) 1% cellulose and PAN blend thin film; (D) 1% cellulose and PAN thin film soaked in DMSO for 5 minutes.

3.4 Conclusions

In this chapter, EMIM Ac and DMSO mixed solvent system was used to achieve a clear combined molecular solution and to blend the cellulose and PAN without microscopic phase separation. The same protocol for spincoating pure cellulose thin films was used for cellulose and PAN blend thin film preparation. The similar viscosity of 1% PAN/3% EMIM Ac/96% DMSO as the 1% cellulose solution makes it suitable for spincoating.

Both blend thin films and pure cellulose thin films showed similar morphology with low roughness and a visual mirror-like surface. The blend thin films of cellulose and PAN maintained excellent stability in hot water and some organic solvents and the same etching resistant to acidic solutions as the pure cellulose thin film. The film resistance in the NaOH/urea system was improved to some extent and no large-scale phase separation between cellulose and PAN was revealed by etching. PAN can be removed with DMSO to create cellulose nanoporous thin film

.

Chapter 4: Conclusions

Cellulose, the most abundant and renewable natural polymer, exhibits excellent chemical and mechanical stability and has wide applications in construction, filtration, bio-scaffolding and packaging. However, due to the effects of hydrophobic interactions between the cellulose layers and the hydrophilic and H-bond interactions associated with -OH groups on the cellulose sugar rings, cellulose dissolution is difficult. Crystallization of cellulose happens when it encounters water molecules, so obtaining a dry molecular solution using an ionic liquid combined with an aprotic organic solvent (DMSO) is the first step to spincoat amorphous thin films. EMIM Ac is suitable solvent for cellulose as the anions and cations are effective at breaking the hydrogen bonds inside the cellulose crystal.

The film morphology is highly sensitive to the preparation conditions so an approximately zero humidity working environment was required. A sealed apparatus filled with dry N_2 gas was constructed to ensure the spincoating process could be conducted in an atmosphere where no water driven crystallization could occur. By in-situ washing with a mixture of acetone and toluene during spincoating, the film surface vitrified before the film was removed from the spincoating apparatus. Afterwards, applied vacuum and acetone soaking was used to further remove DMSO and EMIM Ac and to condense the amorphous cellulose or blend thin films.

FTIR results indicated that DMSO and EMIM Ac were fully removed from the films. (XRD and HR-SFG-VS identified the difference between the amorphous thin film and the original cellulose nanocrystals) The narrow Bragg's peaks in XRD spectrum

confirmed the crystalline regions in original cellulose materials and the broad peaks for cellulose thin films supported the conclusion that the films were amorphous. C-H and O-H stretching vibration frequency regions at ~2951 cm^{-1} and ~3325 cm^{-1} measured by HR-SFG-VS were also supported the amorphous nature of the films. AFM images showed the films exhibited a low roughness morphology independent of the thickness from less than 10 nm to more than 200 nm. The thickness of film can be controlled by either the solution concentration or the initial spincoating speed. XRR was used to evaluate the density of the amorphous thin films as a function of thickness and the effect of EMIM Ac removal by acetone soaking.

Both pure cellulose thin films and blend thin films of cellulose and PAN exhibited stability under harsh solution conditions such as hot water and acidic etching. The blend thin film showed better resistance to the NaOH/urea etching as the thickness decreased more slowly than the pure cellulose film and no large-scale phase separation between cellulose and PAN was observed.

Chapter 5: Future Work

Further investigation on this topic could be to explore a more efficient way to remove IL as the method used in this research was quite time-consuming and the amount of acetone used was large.

Also, more attention should be paid to understand how the worm-like structure formed during soaking in NaOH/urea solution. In addition, reason that PAN with cellulose blends allowed improved the resistance to etching is not understood.

At last, more study should be done on the nanoporous thin films made by using DMSO to dissolve PAN from the blend thin films. This could be a possible route to form membrane materials. Research on controlling the porosity by changing the ratio of cellulose and PAN could be done.

Bibliography

(1) Habibi, Y.; Lucia, L. A.; Rojas, O. J. Cellulose Nanocrystals: Chemistry, Self-Assembly, and Applications. *Chem. Rev.* **2010**, *110*, 3479-3500.

(2) Wada, M.; Nishiyama, Y.; Chanzy, H.; Forsyth, T.; Langan, P. The structure of celluloses. *Powder Diffraction* **2008**, *23*, 92-95.

(3) Huber, T.; Mussig, J.; Curnow, O.; Pang, S. S.; Bickerton, S.; Staiger, M. P. A critical review of all-cellulose composites. *Journal of Materials Science* **2012**, *47*, 1171-1186.

(4) Moon, R. J.; Martini, A.; Nairn, J.; Simonsen, J.; Youngblood, J. Cellulose nanomaterials review: structure, properties and nanocomposites. *Chem. Soc. Rev.* **2011**, *40*, 3941-3994.

(5) Koyama, M.; Helbert, W.; Imai, T.; Sugiyama, J.; Henrissat, B. Parallel-up structure evidences the molecular directionality during biosynthesis of bacterial cellulose. *Proceedings of the National Academy of Sciences* **1997**, *94*, 9091-9095.

(6) Hishikawa, Y.; Togawa, E.; Kataoka, Y.; Kondo, T. Characterization of amorphous domains in cellulosic materials using a FTIR deuteration monitoring analysis. *Polymer* **1999**, *40*, 7117-7124.

(7) Tolonen, L. K.; Penttilä, P. A.; Serimaa, R.; Kruse, A.; Sixta, H. The swelling and dissolution of cellulose crystallites in subcritical and supercritical water. *Cellulose* **2013**, *20*, 2731-2744.

(8) Bledzki, A. K.; Gassan, J. Composites reinforced with cellulose based fibres. *Progress in Polymer Science* **1999**, *24*, 221-274.

(9) Ciolacu, D.; Ciolacu, F.; Popa, V. I. Amorphous cellulose—structure and characterization. *Cellulose chemistry and technology* **2011**, *45*, 13.

(10) Graenacher, C.: Cellulose solution. Google Patents, 1934.

(11) Johnson, D. L.: Compounds dissolved in cyclic amine oxides. Google Patents, 1969.

(12) Swatloski, R. P.; Spear, S. K.; Holbrey, J. D.; Rogers, R. D. Dissolution of cellose with ionic liquids. *Journal of the American Chemical Society* **2002**, *124*, 4974-4975.

(13) Wang, H.; Gurau, G.; Rogers, R. D. Ionic liquid processing of cellulose. *Chem. Soc. Rev.* **2012**, *41*, 1519-1537.

(14) Qi, H.; Sui, X.; Yuan, J.; Wei, Y.; Zhang, L. Electrospinning of Cellulose-Based Fibers From NaOH/Urea Aqueous System. *Macromolecular Materials and Engineering* **2010**, *295*, 695-700.

(15) Han, D. L.; Yan, L. F.; Chen, W. F.; Li, W.; Bangal, P. R. Cellulose/graphite oxide composite films with improved mechanical properties over a wide range of temperature. *Carbohydrate Polymers* **2011**, *83*, 966-972.

(16) Sun, N.; Swatloski, R. P.; Maxim, M. L.; Rahman, M.; Harland, A. G.; Haque, A.; Spear, S. K.; Daly, D. T.; Rogers, R. D. Magnetite-embedded cellulose fibers prepared from ionic liquid. *Journal of Materials Chemistry* **2008**, *18*, 283-290.

(17) Miyauchi, M.; Miao, J.; Simmons, T. J.; Lee, J.-W.; Doherty, T. V.; Dordick, J. S.; Linhardt, R. J. Conductive cable fibers with insulating surface prepared by coaxial electrospinning of multiwalled nanotubes and cellulose. *Biomacromolecules* **2010**, *11*, 2440-2445.

(18) Egorov, V. M.; Smirnova, S. V.; Formanovsky, A. A.; Pletnev, I. V.; Zolotov, Y. A. Dissolution of cellulose in ionic liquids as a way to obtain test materials for metal-ion detection. *Analytical and Bioanalytical Chemistry* **2007**, *387*, 2263-2269.

(19) Liu, S.; Zhang, L.; Zhou, J.; Wu, R. Structure and properties of cellulose/Fe2O3 nanocomposite fibers spun via an effective pathway. *The Journal of Physical Chemistry C* **2008**, *112*, 4538-4544.

(20) Liu, Z.; Li, M.; Turyanska, L.; Makarovsky, O.; Patanè, A.; Wu, W.; Mann, S. Self-assembly of electrically conducting biopolymer thin films by cellulose regeneration in gold nanoparticle aqueous dispersions. *Chemistry of Materials* **2010**, *22*, 2675-2680.

(21) Shi, X. W.; Zhang, L.; Cai, J.; Cheng, G. Z.; Zhang, H. M.; Li, J.; Wang, X. H. A Facile Construction of Supramolecular Complex from Polyaniline and Cellulose in Aqueous System. *Macromolecules* **2011**, *44*, 4565-4568.

(22) Wang, S.; Lu, A.; Zhang, L. Recent advances in regenerated cellulose materials. *Progress in Polymer Science* **2016**, *53*, 169-206.

(23) Chanzy, H.; Maia, E.; Perez, S. Cellulose organic solvents. III. The structure of the N-methylmorpholine N-oxide–trans-1, 2-cyclohexanediol complex. *Acta Crystallographica Section B: Structural Crystallography and Crystal Chemistry* **1982**, *38*, 852-855.

(24) Rosenau, T.; Potthast, A.; Sixta, H.; Kosma, P. The chemistry of side reactions and byproduct formation in the system NMMO/cellulose (Lyocell process). *Progress in polymer science* **2001**, *26*, 1763-1837.

(25) Zhang, H.; Wu, J.; Zhang, J.; He, J. S. 1-Allyl-3-methylimidazolium chloride room temperature ionic liquid: A new and powerful nonderivatizing solvent for cellulose. *Macromolecules* **2005**, *38*, 8272-8277.

(26) Fukaya, Y.; Hayashi, K.; Wada, M.; Ohno, H. Cellulose dissolution with polar ionic liquids under mild conditions: required factors for anions. *Green Chemistry* **2008**, *10*, 44-46.

(27) King, A. W. T.; Asikkala, J.; Mutikainen, I.; Jarvi, P.; Kilpelainen, I. Distillable Acid-Base Conjugate Ionic Liquids for Cellulose Dissolution and Processing. *Angewandte Chemie-International Edition* **2011**, *50*, 6301-6305.

(28) Abe, M.; Fukaya, Y.; Ohno, H. Fast and facile dissolution of cellulose with tetrabutylphosphonium hydroxide containing 40 wt% water. *Chemical Communications* **2012**, *48*, 1808-1810.

(29) Moulthrop, J. S.; Swatloski, R. P.; Moyna, G.; Rogers, R. D. High-resolution C-13 NMR studies of cellulose and cellulose oligomers in ionic liquid solutions. *Chemical Communications* **2005**, 1557-1559.

(30) Remsing, R. C.; Swatloski, R. P.; Rogers, R. D.; Moyna, G. Mechanism of cellulose dissolution in the ionic liquid 1-n-butyl-3-methylimidazolium chloride: a C-13 and Cl-35/37 NMR relaxation study on model systems. *Chemical Communications* **2006**, 1271-1273.

(31) Zhang, J. M.; Zhang, H.; Wu, J.; Zhang, J.; He, J. S.; Xiang, J. F. NMR spectroscopic studies of cellobiose solvation in EmimAc aimed to understand the dissolution mechanism of cellulose in ionic liquids. *Physical Chemistry Chemical Physics* **2010**, *12*, 1941-1947.

(32) Liu, H. B.; Sale, K. L.; Holmes, B. M.; Simmons, B. A.; Singh, S. Understanding the Interactions of Cellulose with Ionic Liquids: A Molecular Dynamics Study. *Journal of Physical Chemistry B* **2010**, *114*, 4293-4301.

(33) Lu, B. L.; Xu, A. R.; Wang, J. J. Cation does matter: how cationic structure affects the dissolution of cellulose in ionic liquids. *Green Chemistry* **2014**, *16*, 1326-1335.

(34) Kontturi, E.; Suchy, M.; Penttila, P.; Jean, B.; Pirkkalainen, K.; Torkkeli, M.; Serimaa, R. Amorphous Characteristics of an Ultrathin Cellulose Film. *Biomacromolecules* **2011**, *12*, 770-777.

(35) Zhang, B. X.; Azuma, J.; Uyama, H. Preparation and characterization of a transparent amorphous cellulose film. *Rsc Advances* **2015**, *5*, 2900-2907.

(36) Johnson, K. E. What's an ionic liquid? *Interface-Electrochemical Society* **2007**, *16*, 38-41.

(37) Sawant, A.; Raut, D.; Darvatkar, N.; Salunkhe, M. Recent developments of task-specific ionic liquids in organic synthesis. *Green Chemistry Letters and Reviews* **2011**, *4*, 41-54.

(38) Kosan, B.; Michels, C.; Meister, F. Dissolution and forming of cellulose with ionic liquids. *Cellulose* **2008**, *15*, 59-66.

(39) Martin, D.; Weise, A.; Niclas, H. J. The solvent dimethyl sulfoxide. *Angewandte Chemie International Edition in English* **1967**, *6*, 318-334.

(40) Food; Administration, D. Guidance for Industry: Q3C–Tables and List. *Rockville, MD: FDA* **2003**.

(41) Scharnagl, N.; Buschatz, H. Polyacrylonitrile (PAN) membranes for ultra-and microfiltration. *Desalination* **2001**, *139*, 191-198.

(42) Kim, D.; Moreno, N.; Nunes, S. P. Fabrication of polyacrylonitrile hollow fiber membranes from ionic liquid solutions. *Polymer Chemistry* **2016**, *7*, 113-124.

(43) Lachat, V. M. Understanding oil resistance of nitrile rubber: CN group interactions at interfaces. University of Akron, 2008.

(44) Scharnagl, N.; Buschatz, H. Polyacrylonitrile (PAN) membranes for ultra- and microfiltration. *Desalination* **2001**, *139*, 191-198.

(45) Guo, H.; Minus, M. L.; Jagannathan, S.; Kumar, S. Polyacrylonitrile/carbon nanotube composite films. *ACS applied materials & interfaces* **2010**, *2*, 1331-1342.

(46) Zhu, G.; Wang, F.; Xu, K.; Gao, Q.; Liu, Y. Study on properties of poly (vinyl alcohol)/polyacrylonitrile blend film. *Polímeros* **2013**, *23*, 146-151.

(47) Anitha, T.; Kumar, P. S.; Kumar, K. S.; Ramkumar, B.; Ramalingam, S. Adsorptive removal of Pb(II) ions from polluted water by newly synthesized chitosan–polyacrylonitrile blend: Equilibrium, kinetic, mechanism and thermodynamic approach. *Process Safety and Environmental Protection* **2015**, *98*, 187-197.

(48) Prasanth, R.; Aravindan, V.; Srinivasan, M. Novel polymer electrolyte based on cob-web electrospun multi component polymer blend of polyacrylonitrile/poly(methyl methacrylate)/polystyrene for lithium ion batteries—Preparation and electrochemical characterization. *Journal of Power Sources* **2012**, *202*, 299-307.

(49) Bochek, A. M.; Murav'ev, A. A.; Novoselov, N. P.; Popova, E. N.; Sazanov, Y. N.; Lavrent'ev, V. K. Composite cellulose-polyacrylonitrile films prepared from solutions in a mixed solvent, 1-butyl-3-methylimidazolium chloride-dimethylformamide. *Russian Journal of Applied Chemistry* **2014**, *87*, 634-639.

(50) Zhang, L.; Lu, Z.; Velarde, L.; Fu, L.; Pu, Y.; Ding, S.-Y.; Ragauskas, A. J.; Wang, H.-F.; Yang, B. Vibrational spectral signatures of crystalline cellulose using high resolution broadband sum frequency generation vibrational spectroscopy (HR-BB-SFG-VS). *Cellulose* **2015**, *22*, 1469-1484.

(51) Schaub, M.; Wenz, G.; Wegner, G.; Stein, A.; Klemm, D. ULTRATHIN FILMS OF CELLULOSE ON SILICON-WAFERS. *Advanced Materials* **1993**, *5*, 919-922.

(52) Yokota, S.; Kitaoka, T.; Wariishi, H. Surface morphology of cellulose films prepared by spin coating on silicon oxide substrates pretreated with cationic polyelectrolyte. *Applied Surface Science* **2007**, *253*, 4208-4214.

(53) Kittle, J. D.; Wang, C.; Qian, C.; Zhang, Y. F.; Zhang, M. Q.; Roman, M.; Morris, J. R.; Moore, R. B.; Esker, A. R. Ultrathin Chitin Films for Nanocomposites and Biosensors. *Biomacromolecules* **2012**, *13*, 714-718.

(54) Yeng, L. C.; Wahit, M. U.; Othman, N. THERMAL AND FLEXURAL PROPERTIES OF REGENERATED CELLULOSE (RC)/POLY (3-HYDROXYBUTYRATE)(PHB) BIOCOMPOSITES. **2015**.

(55) Wang, H.-F.; Velarde, L.; Gan, W.; Fu, L. Quantitative sum-frequency generation vibrational spectroscopy of molecular surfaces and interfaces: lineshape, polarization, and orientation. *Annual review of physical chemistry* **2015**, *66*, 189-216.

(56) Zhang, L. N.; Ruan, D.; Zhou, J. P. Structure and properties of regenerated cellulose films prepared from cotton linters in NaOH/Urea aqueous solution. *Industrial & Engineering Chemistry Research* **2001**, *40*, 5923-5928.

(57) Qi, H. S.; Yang, Q. L.; Zhang, L. N.; Liebert, T.; Heinze, T. The dissolution of cellulose in NaOH-based aqueous system by two-step process. *Cellulose* **2011**, *18*, 237-245.

(58) Xiong, B.; Zhao, P. P.; Hu, K.; Zhang, L. N.; Cheng, G. Z. Dissolution of cellulose in aqueous NaOH/urea solution: role of urea. *Cellulose* **2014**, *21*, 1183-1192.

(59) P.A. Kienzle, K. V. O. D., J.F. Ankner, N.F. Berk, C.F. Majkrzak. http://www.ncnr.nist.gov/reflpak. **2000-2006**.

(60) Rein, D. M.; Khalfin, R.; Szekely, N.; Cohen, Y. True molecular solutions of natural cellulose in the binary ionic liquid-containing solvent mixtures. *Carbohydrate Polymers* **2014**, *112*, 125-133.

(61) Zugenmaier, P. Materials of cellulose derivatives and fiber-reinforced cell ulose-polypropylene composites: Characterization and application. *Pure and Applied Chemistry* **2006**, *78*, 1843-1855.

(62) Fu, L.; Wang, W.; Yu, L. J.; Zhang, S. M.; Yang, G.: Fabrication of Novel Cellulose/Chitosan Artificial Skin Composite. In *Materials Research, Pts 1 and 2*; Gu, Z. W., Han, Y. F., Pan, F. H., Wang, X. T., Weng, D., Zhou, S. X., Eds.; Materials Science Forum, 2009; Vol. 610-613; pp 1034-1038.

(63) Lv, J.; Zeng, D. M.; Wei, C. Mechanical and Wear Properties of Sisal Fiber Cellulose Microcrystal Reinforced Unsaturated Polyester Composites. *Advances in Polymer Technology* **2015**, *34*.